

NATIONAL AERONAUTICAL ESTABLISHMENT
LIBRARY

C P. No. 154
(15,361)
A R C Technical Report



26 AUG 1954

MINISTRY OF SUPPLY

AERONAUTICAL RESEARCH COUNCIL

CURRENT PAPERS

The Rapid, Accurate Prediction of Pressure on
Non-Lifting Ogival Heads of Arbitrary Shape,
at Supersonic Speeds

By

B. W. Bolton-Shaw and H. K. Zienkiewicz
of the English Electric Co.
Navigational Project Division, Luton

LONDON HER MAJESTY'S STATIONERY OFFICE

1954

FIVE SHILLINGS NET



ADDEDUM

Since the above paper had been written further work has been done by the writer on the various methods developed in the main body of the paper. It is hoped that a detailed report on this further work will be published in the near future (Ref. AD.1); meanwhile the following summarises those results of the work that affect applicability of the methods presented here.

1. The Ogive of Curvature Method

(1) Comparison of results of this method with experiment and with pressure distributions calculated by the method of characteristics on a number of head shapes, with large nose angles and at Mach numbers such that the loss of stagnation pressure across the nose shock wave was up to 30% of the free stream stagnation pressure, has led to the conclusion that the basic assumption of the ogive of curvature method (para. 2. 3, p.7) should be modified to read:

"The ratio of the local static pressure to the free-stream static pressure at a point P on an arbitrary convex head at a free stream Mach number M is the same as at P on the ogive of curvature at P at the same free stream Mach number M."

The comparisons with van Dyke's method, shown in figs. 9 and 10 are not significantly affected by this modification of the basic assumption, since in all cases considered there the stagnation pressure loss across the nose shock was sufficiently low for the two forms of the assumption to be effectively equivalent.

(ii) To deal with the cases where the nose angle of the ogive of curvature becomes so small that λ cannot be obtained from fig. 1, the $\lambda - x$ chart has been extended down to $K = 0.1$. It can be shown that $\lambda \rightarrow 0$ as $x \rightarrow 0$, hence in fig. 1 the local trend near $K = 0.4$ would lead to serious errors if used for extrapolating the variation of λ with x to lower values of K . The extended $\lambda - x$ chart (at present in a provision form) will be found in Ref. Ad.1.

Some experimental results verifying the modified ogive of curvature method and the extended $\lambda - x$ chart are published in ref. AD.2.

2. The Log $p \sim \theta$ Law

The theoretical and experimental results mentioned above indicate that if over a region of a head $2M \tan \frac{x}{2} < 0.4$, approx, the log $p \sim \theta$ law will be in error over and downstream of such a region. If this occurs towards the rear of the head, where the slope is small, the resulting error in the wave drag coefficient may not be serious, but otherwise the log $p \sim \theta$ law should not be used unless $2M \tan \frac{x}{2} > 0.4$ everywhere on the head.

3. The Derivative Formula

In view of the assumptions and approximations involved in its derivation this formula can be expected to give reasonable accuracy only if $0.4 < 2M \tan \frac{x}{2} < 1.0$, approx,

4. A Step-by-Step Method.

Effects of large stagnation pressure losses across the nose shock, on the accuracy of the step-by-step method have not yet been investigated, nor has the extended $\lambda - x$ chart been used with this method.

Additional References

<u>No.</u>	<u>Author(s)</u>	<u>Title, etc.</u>
Ad.1	Zienkiewicz, H. K.	Further development of some approximate methods of predicting pressures on non-lifting ogival heads of arbitrary convex shape, at supersonic speeds. To be published as an English Electric Co., LA.t. Report.
Ad.2	Marson, Keates and Socha	An experimental investigation of the pressure distribution on five bodies of revolution at Mach numbers of 2.45 and 3.19. College of Aeronautics Report No.79, 1954.

The Rapid, Accurate Prediction of Pressure on
Non-Lifting Ogival Heads of Arbitrary Shape,
at Supersonic Speeds.

- By -

B. W. Bolton-Shaw and H. K. Zienkiewicz.

The English Electric Co., Ltd., Navigational Project Division, Luton
Report No. LA.t.034

23rd June, 1952

Summary

Five methods are developed for determining the pressure distribution on an arbitrary, pointed, convex axi-symmetric head shape, of which the ordinate and its first three derivatives are everywhere continuous. When the geometric details are specified, the time required to pressure plot a head shape by these methods is from approximately 20 minutes to 3 hours. The methods were checked in five trial cases against accurate pressure distributions, obtained by using van Dyke's second order theory, and generally gave very good agreement. The best method to use of the five depends on head shape and on the speed and accuracy required, and recommended methods are given.

These recommended methods are greatly superior in accuracy to linearised theory, and in rapidity of computation to both the method of characteristics and van Dyke's second order theory. C_p is predicted to within $\pm 2\%$ of the value of C_p at the nose, provided the effects of rotation produced by the curved shock are negligible and provided the radius of curvature is not infinite at the point of zero slope.

Two of these methods can be readily applied to determine minimum drag head shapes. This application will be described in a subsequent

report. The methods are also of use when obtaining accurate values of lift, etc. of bodies at incidence by the hybrid theory proposed by van Dyke.

It may be possible to adapt the methods of this report to apply to ducted bodies of revolution. A possible approach is suggested.

List of Contents.

	Page.
List of Symbols	2
ξ1. Introduction	4
ξ2. The Five Methods of Predicting Pressures	5
2.1. The Fundamental Assumption.	5
2.2. The λ Step-by-Step Method for Arbitrary Profiles.	7
2.3. The Ogive of Curvature Method	7
2.4. The Derivative Formula Method.	9
2.5. The Log $p \sim 0$ Law	9
2.6. The Effects of Rotation	10
ξ3. Bodies at Incidence	11
ξ4. Application of the Theory to Ducted Bodies of Revolution.	12
ξ5. Appraisal of the Five Different Methods and Comparison with Solutions by Van Dyke's Second Order theory.	13
5.1. The λ Step-by-Step Method.	14
5.2. The Ogive of Curvature Method Using L.A.t.024 (Ref.4)	15
5.3. The Ogive of Curvature Method Using NACA T.N.2250 (Ref.6)	16
5.4. The Derivative Formula.	16
5.5. The Linear Log $p \sim 0$ Law	17
5.6. Merits and Limitations of the Five Methods.	17
ξ6. Conclusions	22
References	24
Appendices I - IV.	25 - 44
Figures 1 - 13.	

List of Symbols.

$$C_p = \frac{p - p_0}{0.7 M^2 p_0}, \text{ pressure coefficient}$$

D maximum diameter of body

- $F(\nu)$ ratio of static to stagnation pressure after Prandtl-Meyer expansion through angle ν from sonic velocity
- $G(v_A)$ function of v_A defined by equation (iii), Appendix I
- $k = \sigma \log_e 10$
- $K = \left(\frac{L}{D}\right)$
- L length of a body
- $m = \frac{-d(\log_{10} p)}{dx}$ for circular arc ogives
- M free stream Mach number of flow past arbitrary body
- \bar{M} free stream Mach number of flow past ogive of curvature
- M_L local Mach Number
- M_N surface Mach number just downstream of nose shock
- p surface static pressure
- p_0 free stream static pressure
- p_{stag} surface stagnation pressure
- p_{stag_0} free stream stagnation pressure
- P per cent head length of a point on a circular arc tangent ogive
- R maximum radius of body
- x abscissa of point on arbitrary body, measured from nose, parallel to body axis, and expressed as a fraction of L
- y ordinate of point on arbitrary body, measured as perpendicular distance from body axis, and expressed as a fraction of L
- $y_1 = \frac{dy}{dx}$
- $y_2 = \frac{d^2y}{dx^2}$
- γ ratio of specific heats of gas flowing past body
- $\Delta \lambda = \lambda_1 - \lambda_2$
- θ angle between body axis and tangent to body profile
- θ_S nose semi-angle of body
- λ parameter occurring in equation (1) of § 2
- λ_1 value of λ given by equation (iii), Appendix I
- λ_2 value of λ derived from Fig.6
- ν angle between flow direction and sonic flow direction, in Prandtl-Meyer expansion

ρ radius of curvature of body profile

$\sigma = \frac{d(\log_{10} p)}{d\theta}$ in axi-symmetric flow

$\phi = X_P - \theta_P$

X nose semi-angle of ogive of curvature or of circular arc ogive

ω angle defined by: $F(\omega) = \left(\frac{p}{p_{stag}} \right)_P$

Suffices.

- A conditions at nose A of ogive of curvature at point P
- A - S conditions in axi-symmetric flow past a profile
- N conditions at surface just downstream of nose (or leading edge) shock
- P conditions at current point P on surface.
- Q conditions at point Q on surface, adjacent to P
- 2 - D conditions in two dimensional flow past a profile

§1. Introduction

There are at present three methods of pressure plotting a non-lifting body of revolution of arbitrary shape at supersonic speeds:

- (i) van Dyke's Second Order theory (refs. 1 and 2) which gives accurate results over a wide range of Mach numbers and nose angles, after a minimum of about 20 hours computing time per body per Mach number.
- (ii) The Method of Characteristics which gives accurate results after about one week's computing, unless automatic programmed computing machines (such as Eniac) are used. When such machines are used the time of initial preparation is of the order of several weeks.
- (iii) The First Order theory of von Karman and Moore (ref.3). When the body cross-sectional area is a simple polynomial function of the distance from the nose, the pressure distribution can be calculated in an hour or less. The accuracy of this method decreases rapidly with decrease of fineness ratio. At $M = 2$ the theory underestimates the C_p of 10° and 20° semi-angle cones by 15% and 34% respectively (see Fig.2, ref.2). The error increases with Mach number.

For the purpose of determining the projectile shape of minimum wave drag or simply for pressure plotting an existing projectile shape methods (i) and (ii) are very lengthy and (iii) is too inaccurate. In this report several methods of pressure plotting an arbitrary head shape are given which are free from these defects and which give excellent agreement in C_p with accurate solutions obtained by van Dyke's Second Order theory, for a number of profiles covering a wide range of different distributions of slope along the head.

§2. The Five Methods of Predicting Pressure.

2.1. The Fundamental Assumption

In ref. 4 it is shown that in non-lifting supersonic flow past circular arc ogival heads there is a simple proportionality between the decrease in pressure from the nose to a point P on the profile and the decrease in pressure from the leading edge of an airfoil section of the same profile to the same point P, when the local Mach numbers and pressures just downstream of the leading edge and of the nose are the same. If p_p is the static pressure at point P, p_N the surface static pressure just downstream of the nose,

$$(p_N - p_p)_{A-S} = \lambda (p_N - p_p)_{2-D} \quad \dots \dots \dots (1)$$

where suffices A-S and 2-D refer to axi-symmetric and two-dimensional flows past the same profile, with the same surface pressure and Mach number, p_N and M_N , just behind the shock. λ depends solely on the free stream Mach number and the particular circular arc profile concerned, and is plotted in Fig.1 of this report. (This figure supersedes Fig. 3 of ref. 4. It extends the latter to $K = 0.4$). This simple relation (1) holds, as shown in ref. 4, to within about $\pm 2\%$ accuracy for a very wide range of circular arc profiles and free stream Mach numbers.

The question arises whether the law of expansion (1) would hold for non-circular profiles. For tangent circular arc ogives, λ depends on the radius of curvature of the profile expressed non-dimensionally in units of the calibre (or length) of the tangent ogive. It would therefore be expected that on a profile of continuously varying radius of curvature, λ would also continuously vary.

It is assumed, as the basis of a method for predicting pressures on an arbitrary head shape, that the flow in expanding along the profile from a point P to the adjacent point Q (see Fig.2) expands as if the body were replaced by the ogive of curvature at P (i.e. the ogive generated by the revolution about the axis of an arc of the circle of curvature at P.) Thus the value of λ to use at P in equation (1) is that corresponding to the ogive of curvature at P. This assumption is an arbitrary one, but it gives the pressure exactly in three particular cases:

(i) Flow Past Cones

In this case the profile is a straight line so that

$(p_N - p_P)_{2-D}$ is everywhere zero and equation (1) gives:

$(p_P)_{A-S} = (p_N)_{A-S}$. (The value of $(p_N)_{A-S}$ is determined from the nose angle and Mach number, using the Tables of ref. 5).

(ii) Flow Past Circular Arc Ogives.

The assumption here is exactly true, since the ogive of curvature coincides with the body itself.

(iii) Flow Just Downstream of the Nose of Any Ogive.

The pressure gradient at the nose of a body at a given Mach number is determined solely by the slope and radius of curvature at the nose. The body and the ogive of curvature have the same slope and radius of curvature at their common point, so the fundamental assumption will give the correct pressure gradient at the nose for any body shape. The method also correctly gives the nose pressure as the pressure on a cone of the same nose angle.

Since the fundamental assumption gives the correct pressure and pressure gradient at the nose of any head and gives the correct pressure along the entire head when the profile slope varies effectively; uniformly along the head (circular arc ogives) or is constant (cones), it is reasonable to hope that the fundamental assumption will give fairly accurate pressure distributions along any head.

The basis of the first method of pressure prediction is to find the pressure just behind the nose shock by the Tables of ref.5 and with this starting value to proceed a short distance along the head and obtain

the next value of pressure by equation (1) and the fundamental assumption. The pressure distribution is thus established, step-by-step, along the head. The details of this procedure are given in the following section 2.2 and in Appendix I.

2.2. The λ Step-by-Step Method for Arbitrary Profiles.

Suppose the flow has been traced up to the point P in Fig.2, by some means. Then the static pressure p_p and stagnation pressure p_{stag_p} at P are known. The value of λ at P for the expansion from P to the next point Q, close to P, is that corresponding to the ogive of curvature at P and to some hypothetical free-stream Mach number \bar{M} , which is such that when the ogive of curvature is placed in a uniform flow at Mach number \bar{M} the ratio of static to stagnation pressures at P is $\frac{p_p}{p_{stag_p}}$. There is only one Mach number \bar{M} satisfying this condition and the method of determining λ and \bar{M} is explained in Appendix I. (It was discovered empirically that \bar{M} was always the same (within the reading error of the graphs used, i.e. about 0.005) as the free stream Mach number M of the flow past the body, and this discovery forms the basis of a second, more rapid method of pressure prediction described in 2.3.)

Having obtained λ by the procedure of Appendix I, the change in $\frac{p}{p_{stag}}$ over the short finite interval PQ is calculated, knowing $\left(\frac{p}{p_{stag}}\right)$ at the beginning of the interval, from:

$$\Delta \left(\frac{p}{p_{stag}} \right)_{A-S} = \lambda \Delta \left(\frac{p}{p_{stag}} \right)_{2-D}$$

The details of this calculation are also given in Appendix I. Thus $\frac{p}{p_{stag}}$ and hence C_p can be found by this step-by-step process at a number of points spaced along the head. If required, a second approximation can be obtained as explained in Appendix I. In practice, a second approximation is unnecessary unless the head shape has very rapid curvature at some point. Each C_p requires about 30 minutes calculation.

2.3. The Ogive of Curvature Method.

As stated in the preceding section, it was discovered empirically, when applying the λ step-by-step method, that the ratio of static to stagnation pressure at a point P on an arbitrary body at free stream

Mach number M is the same as at P on the ogive of curvature at P at the same free stream Mach number M.

Since the pressures on the ogive of curvature can be determined by the methods of either ref.4 or ref.6 (p.9), the pressures on any ogival head can be calculated. The only information that is required about the geometry of the arbitrary head is the distributions along the head of the head surface inclination θ to the axis and of the nose semi-angle χ of the ogive of curvature. In terms of rectangular cartesian co-ordinates x and y of the head profile (see Fig. 2), the derivatives y_1 and y_2 and the radius of curvature ρ , it will be readily verified that these angles are given by:

$$\theta = \tan^{-1} y_1$$

$$\chi = \cos^{-1} \left\{ \cos \theta - \frac{y}{\rho} \right\}$$

$$= \cos^{-1} \left\{ \cos \theta (1 + y y_2 \cos^2 \theta) \right\}$$

(Since θ decreases along the head, which is assumed convex, y_2 is -ve and $\rho = -y_2^{-1} (1 + y_1^2)^{3/2}$.)

Once these angles have been determined the method described in ref. 4 can be applied to determine $\frac{p}{p_{\text{stag}}}$ and hence C_p at any point on the arbitrary profile. (In ref. 4, the notation differs slightly in that θ_s replaces χ .) The time required to pressure plot an arbitrary head shape by this procedure, after θ and χ have been calculated, is approximately 90 minutes. A worked example of this procedure is given in Appendix II.

Alternatively in fig. 6 of ref. 6, generalised curves are given of the distribution of $\left\{ \frac{p - p_0}{p_0} \right\}$ over tangent circular arc ogives as a function of the per cent head length and the similarity parameter K (the ratio of Mach number to the fineness ratio of the tangent circular arc ogive.) These curves are reproduced in Figs. 3a ($0.3 \leq k \leq 1.0$) and 3b ($1.0 \leq k \leq 2.0$), for the convenience of the reader. (A van Dyke second order solution for the flow past a circular arc ogive was calculated at $K = 0.4$ and those values of $\left\{ \frac{p}{p_0} - 1 \right\}$ have been used to extend the curves to $K = 0.4$. They are extrapolated to $K = 0.3$, bearing in mind that for a needle-like body, i.e. $K = 0$, $\left\{ \frac{p}{p_0} - 1 \right\} \equiv 0$.) The per cent head length and

similarity parameter of the ogive of curvature are given by:

$$\text{per cent head length} = 100 \left(1 - \frac{\sin \theta}{\sin \chi} \right)$$

$$K = 2M \tan \frac{\chi}{2}$$

For values of χ up to 20° , the following simplified, approximate formula can be used, involving less than $\frac{3}{4}\%$ error:

$$\text{per cent head length} = 100 \left(1 - \frac{\theta}{\chi} \right)$$

After the distributions of θ and χ along the arbitrary body have been determined, the above quantities are calculated and the corresponding values of $\left\{ \frac{p - p_0}{p_0} \right\}$ are read from Fig. 3. Hence $\frac{p}{p_{\text{stag}}}$ and hence C_p . The time required to pressure plot a head shape by this procedure, after θ and χ have been calculated, is about 40 minutes. This procedure, although quicker than using the method of ref. 4, is not quite as accurate. The reason for this is that the curves of Fig. 3 are derived from mean curves through a large number of points, obtained by the method of characteristics for various circular arc ogives at various Mach numbers, which are scattered slightly about the mean curves. The accuracy of both procedures is compared with that of van Dyke's Second Order Theory in §5. An illustrative example of the application of both procedures is given in Appendix II.

2.4. The Derivative Formula Method.

By means of the results of ref. 6, it is possible to deduce an analytic formula in terms of χ and θ , and hence in terms of y , y_1 and y_2 , for the pressure distribution on an arbitrary head shape. This formula and its derivation is given in Appendix III. It involves some further approximations, but nevertheless gives quite accurate values of C_p . The prime purpose of its derivation was the calculation of the projectile shape of minimum wave resistance, by the Calculus of Variations. This work will be reported in a later report.

2.5. The Linear $\log p \sim \theta$ Law.

It soon became apparent that the shape of the pressure distribution curves closely resembled the shape of the slope

distribution curves. Convexities and concavities and points of inflexion in one were always reproduced in the other. It therefore, appeared that slope and pressure were closely related. In ref. 6, it is shown that the pressure decays exponentially with distance along circular arc ogival heads. Since slope varies effectively linearly with distance along a circular arc ogival head (when the nose angle is less than 20°), therefore the pressure decays exponentially with slope. A check showed in all cases considered that the pressure decayed exponentially with slope on non-circular, ogival heads also. Thus a plot of $\log_{10} p$ vs. θ would be a straight line, of gradient σ , say. The gradient, at the nose, of a $\log_{10} p$ vs. θ plot is derivable from the differential form of equation (1):

$$dp_{A-S} = \lambda dp_{2-D}$$

and from the Prandtl-Meyer relation. The details of the derivation are given in Appendix IV and σ so derived, viz. $0.0106 \sqrt{\frac{\lambda_N M_N^2}{M_N^2 - 1}}$,

is plotted as a function of θ_s and M in Fig. 4. The pressure at any point is then given by the formula:

$$\log_{10} \left(\frac{p_N}{p} \right) = \sigma(\theta_s - \theta) \dots \dots \dots (2)$$

where θ_s is the nose semi-angle of the head and p_N the surface static pressure just downstream of the shock, obtained from ref.5. (In this formula θ and θ_s are measured in degrees when multiplied by the values of σ given in Fig. 4). This method requires about 20 minutes to pressure plot a head shape, once the distribution of θ has been determined.

Equation (2) may also be recast in approximate, derivative form for minimum drag shape calculations, thus:

$$p = A e^{k y_1}$$

where: $k = 2.303\sigma$ (σ now measured in rad^{-1})

and $A = p_N e^{-k [y_1]_N}$

2.6. The Effects of Rotation.

The five methods developed in the previous section are all based

on pressure distributions on circular arc ogives calculated by the method of characteristics in ref. 6. These calculations were carried out on the assumption of irrotational flow and neglect changes of entropy along the nose shock wave. Thus none of the methods of the present report is applicable at high K , i.e. either to thick bodies or to very high Mach numbers, for then the effects of rotation caused by the curvature of the nose shock wave, are appreciable. The magnitude of these effects can be ascertained from ref. 10 in which the pressure distributions of ref. 6 on circular arc tangent ogives are recalculated taking account of the rotation of flow. It is found that at $K = 1$ the neglect of rotation results in underestimating C_p over most of the head length by about 2% of C_{pN} ; $\frac{\Delta C_D}{C_D}$, the corresponding error in the wave drag coefficient, is about 6%. The effect of rotation is zero at $K = 0$ and at first increases very slowly with K , as shown in the following table:

K	0.5 - 0.6	0.7	0.8	0.9	1.0	2.0
$\frac{\Delta C_D}{C_D}$	< 0.010	0.010	0.020	0.035	0.060	0.280

Thus, for $K \leq 0.8$ the effect of rotation on $\frac{C_p}{C_{pN}}$ and on C_D will

not exceed one or two per cent, and at $K = 1$ rotation will probably increase C_p by about 2% of C_{pN} and C_D by about 6% above their predicted values. Above $K = 1$, it is expected that the methods of this report, by neglecting rotation, would introduce errors in C_D that may be as large as, say, 30%. For all the head shapes pressure plotted in Figs. 8 - 13, K lies between 0.4 and 0.7.

§3. Bodies at Incidence.

For supersonic bodies of revolution at incidence, van Dyke suggests in ref. 1. that to obtain accurate values of lift, pressure, etc, it is necessary to calculate the surface velocity components in non-lifting flow to the accuracy of van Dyke's second order theory and to superpose on these the cross flow surface velocity components obtained from first order theory. The theory of this report is therefore of direct application

in determining the non-lifting flow surface pressures and hence those non-lifting flow surface velocity components, required for such a "hybrid" theory.

§4. Application of the Theory to External Flow Past Ducted Bodies of Revolution.

Consider the external flow past a ducted conical frustrum of semi-angle θ_s , when the external shock is attached to the mouth. The mouth pressure is that corresponding to a two-dimensional plane shock for a wedge angle θ_s . This pressure is considerably higher than that on a cone of semi-angle θ_s . Far downstream of the mouth, the pressure on the frustrum becomes independent of local conditions at the mouth. Thus the pressure on the frustrum falls asymptotically from the two-dimensional wedge pressure occurring at the mouth to the pressure on a cone of semi-angle θ_s .

Similarly the external pressure on an arbitrary ducted body with attached external shock will fall asymptotically from the two-dimensional wedge pressure occurring at the mouth to the pressure that would occur if the profile were extended upstream from the mouth to a sharp point. The pressure distribution by the methods of this report when applied to the body extended to a sharp point, will therefore approach asymptotically the correct pressure distribution. The mouth pressure can be exactly calculated from plane shock relations, but the pressures predicted by the methods of this report will only become accurate at some finite relaxation distance from the mouth, where the local effect of the mouth has sufficiently decayed. In the only case the authors have so far investigated, in which the pressures by the methods of this report were compared with pressures by van Dyke's second order theory on a convex ducted body at $M = 2.0$, this relaxation distance was 2 mouth diameters and consequently a large and important part of the pressure distribution curve could not be accurately predicted.

Before the methods of this report can be modified to apply over the relaxation distance, information must be obtained about external pressure distributions on ducted conical frustra. It may then be possible to predict accurately the pressure everywhere on a ducted body, of mouth semi-angle θ_s at Mach number M , as the sum of the pressure by the methods of this report and a pressure, sufficient to give the correct value at the mouth, which decays to zero in the same way as for a ducted conical frustrum,

$$\text{i.e. } C_p = C_{p1} + k (C_{p2} - C_{p3})'$$

$$\text{where: } k = \frac{C_{p4} - (C_{p1})_n}{C_{p4} - C_{p3}} \quad (\text{in practice } k \text{ is nearly } 1)$$

C_{p1} = pressure coefficient at M predicted by the methods of this report when the body is extended to a sharp point

$(C_{p1})_n$ = value of C_{p1} at the mouth

C_{p2} = pressure coefficient at M on conical frustrum, tangential to the ducted body at their common mouth

C_{p3} = pressure coefficient at M on cone with semi-angle θ_s

C_{p4} = pressure coefficient at M corresponding to plane shock with wedge angle θ_s

This formula for C_p would give the correct mouth pressure, $C_p = C_{p4}$, and the correct asymptotic pressure distribution, $C_p = C_{p1}$, a long way back along the head. Also the relaxation distance is the same as for the conical frustrum associated with C_{p2} , which is a reasonable assumption. The formula would give the exact pressure distribution on a conical frustrum.

However the authors have not yet developed this approach and until this has been done, the methods of this report are of little help in predicting the external pressure distributions on a ducted body with attached external shock.

5. Appraisal of the Five Different Methods and Comparison with Solutions by van Dyke's Second Order Theory.

The five different methods described in §2 were used to calculate pressure distributions on the following heads:

1. $y = \frac{1}{6} \left\{ 1 - (1-x)^{1.5} \right\}$ at $M = 2.0$, $L/D = 3$, $K = 0.667$;
2. $y = \frac{1}{6} \left\{ 1 - (1-0.6x)^3 \right\}$ at $M = 2.0$, $L/D = 3$, $K = 0.667$;
3. $y = 0.1889 x^5 - 0.5634 x^4 + 0.7560 x^3 - 0.4670 x^2 - 0.02504 x + 0.3963 \left[1 - (1-x)^{1.5} \right]$, at $M = 2.0$ $L/D = 3.5$, $K = 0.571$

This profile was derived by modifying the slope distribution of

Lighthill's "minimum drag" ogive (ref. 9) over the first 15% of the head length to obtain a pointed nose, and then following the slope distribution very closely along the rest of the head.

$$4. \quad y = 0.03968 (\pi x + \sin \pi x), \text{ at } M = 1.6 \text{ and } 2.8, \frac{L}{D} = 4, K = 0.400$$

and 0.700

$$5. \quad y = \frac{1}{8} \left[1 - (1 - x)^3 \right], \text{ at } M = 2.0, \frac{L}{D} = 4, K = 0.500$$

For comparison, solutions were also obtained for heads 1, 2, 3, and 4 at Mach numbers as stated above, by the second order theory of van Dyke. As is shown in ref. 1 (p.p. 167-170), this theory gives excellent agreement with the exact inviscid solutions for ogives (the method of characteristics) and cones (Taylor-Maccoll). This is further borne out in the present investigation, by the agreement in C_{PN} between the second order and the exact values, which is within 1% in all the cases investigated except for head 4 at $M = 2.8$, where C_{PN} is overestimated by 2%. Consequently, the second order solutions are here considered to give the inviscid pressure distributions exactly, and are used as a standard for assessing the accuracy of the five methods.

Fig. 7 shows the profiles and the slope distributions of these five heads. The head profiles were chosen so that a wide variety of types of slope distributions would be represented—as is seen from Fig. 7, the curves of $\tan \theta (= \frac{dy}{dx})$ vs. x are concave, convex and inflexional (changing both from concave to convex and vice versa). It is to be noted that the slopes become zero at $x = 1$ in all cases with the exception of head 2, which is a secant ogive. Further, at $x = 1$ the radii of curvature of heads 1 and 3 are zero, those of heads 4 and 5 are infinite, whilst head 2 terminates with a finite radius of curvature. The significance of this becomes apparent in section 5.6.

5.1. The λ Step-by-Step Method.

The pressure distributions on heads 1 - 4 obtained by this method are shown in Fig. 8 compared with those calculated by van Dyke's second order theory.

It is seen that for heads 1, 2 and 3 the agreement between the two methods is excellent. The step-by-step method reproduces very closely the shapes of the second order pressure distributions.

There are slight discrepancies in the magnitudes of C_p , but these amount to no more than 2% of the corresponding C_p values at the nose (C_{pN}) and may be attributed partly to the inaccuracies of the van Dyke solutions at the nose, as compared with the exact Taylor-Maccoll values which were used in the step-by-step method.

In the case of head 4 at $M = 2.8$, the step-by-step method gives accurate results over the first 70% of the head length. Beyond $x = 0.7$, the method overestimates expansion and takes no account of the slight recompression which appears to occur over the last 15% of the head length. At about $x = 0.94$, the method ceases to give results since the values of χ fall outside the range of fig. 6. On the same head at $M = 1.6$, the agreement is excellent over the first 40% of the head length. The divergence between the two methods begins at $x = 0.4$ approximately, the step-by-step method in this case overestimating C_p by amounts of up to 7% of C_{pN} . These discrepancies may partly be due to the fact that the values of λ as a function of χ determined in ref. 4. are less reliable for $M = 1.6$ than they are for higher Mach numbers (2 and over). At $M = 1.6$, calculations by the step-by-step method cannot be carried beyond about $x = 0.8$ on this head.

5.2. The Ogive of Curvature Method Using L.A.t.024 (Ref.4)

Fig. 9 shows pressure distributions on heads 1 - 4 predicted by the ogive of curvature method, using L.A.t.024.

Comparison of figs. 9 and 8 reveals that the pressure distributions calculated for heads 1, 2 and 3 and head 4 at $M = 1.6$ by this method are practically identical with those obtained by the step-by-step method, and hence give equally good agreement with the second order solutions. On head 4 at $M = 2.8$ the two methods agree closely as far as $x = 0.4$ and then begin to diverge, the difference between them increasing along the head. Thus, it appears that the hypothesis which forms the basis of the ogive of curvature method, (viz. that the ratio of static pressure to stagnation pressure at a point P on an arbitrary body at a free stream Mach number M is the same as at P on the ogive of curvature at P at the same free stream Mach number M - see sections 2.1., 2.2 and 2.3), is borne out in the case of heads 1, 2 and 3 and head 4 at $M = 1.6$, but does not hold

with the same accuracy for head 4 at $M = 2.8$. Now, the distribution of χ on head 4 is such that at $M = 2.8$ the maximum difference between the stagnation pressure losses across the conical shocks of the body and of the ogive of curvature is, approximately, 2% of the free stream stagnation pressure. On the other heads and on head 4 at $M = 1.6$, stagnation pressure losses did not exceed $\frac{1}{2}\%$. This suggests that the hypothesis on which the ogive of curvature method is based becomes less accurate as the difference increases between the stagnation pressure loss for the ogive of curvature and the corresponding loss for the body.

5.3. The Ogive of Curvature Method using NACA TN.2250 (Ref. 6)

The pressure distributions predicted by the ogive of curvature method using NACA TN.2250 instead of L.A.t.024 are shown in Fig.10. Although the two procedures are basically equivalent, the use of curves of ref. 6 results in a slight loss of accuracy for reasons explained in Section 2.3. Nevertheless, the agreement with the second order solutions is still good. In the case of heads 1, 2 and 3, the predicted C_p 's do not differ from the second order C_p 's by more than about $\pm 3\%$ of C_{pN} , the discrepancies being greatest near the nose. On head 4 at $M = 2.8$, C_p appears to be underestimated by about 3% of C_{pN} over most of the head; at $M = 1.6$, C_p near the nose is again underestimated by some 3%, whilst for $x > 0.5$ the error is roughly one and a half times that of the more accurate methods discussed in sections 5.1 and 5.2.

5.4. The Derivative Formula.

Fig.11 shows the pressure distributions calculated by the derivative formula given in Appendix III.

Apart from the singular behaviour beyond about $x = 0.98$ on heads 1 and 3, this formula predicts the pressure distributions on heads 1, 2 and 3 with errors not greater than + 4% of C_{pN} . The obvious failure of the method when it predicts perfect vacuum at $x = 1$ on heads 1 and 3 can be traced back to the approximations involved in the derivation of the formula. In particular, χ is approximated by

$$X = \sqrt{y_1^2 - 2yy_2} \quad \left[\text{Eqn. (ix) App. III} \right]$$

which involves the assumption that y/λ is small. Now on heads 1 and 3, $\eta \rightarrow 0$ ($y_2 \rightarrow -\infty$) as $x \rightarrow 1$, whilst y remains finite and so the above assumption is not satisfied. According to the theory of the derivative formula, $X \rightarrow \infty$ as $x \rightarrow 1$, (in fact, X cannot be determined there, being an angle whose cosine exceeds unity), and $\frac{p}{p_0} \rightarrow 0$, so that a perfect vacuum is obtained.

On head 4 at $M = 2.8$ a very good agreement (within about $\pm 2\%$ of C_{pN}) with van Dyke's solution is obtained, except near the end of the head, where at $x = 1$ the derivative formula predicts a small positive C_p . On the same head at $M = 1.6$ the formula underestimates C_p near the nose by about 4%, overestimates it over the rear part of the head and exaggerates the recompression near the end. The wide disagreement over the last 10 or 20% of the head length and the prediction of a small positive C_p at $x = 1$ is due to the fact that the representation of n and $\log \left(\frac{p}{p_0} \right)_N$ as linear functions of K (see Appendix III) holds only for K between 0.5 and 1 and is not a good approximation for $K < 0.4$, which is the case on head 4 as the end of the head is approached.

5.5. The Linear Log $p \sim \theta$ Law.

The pressure distributions calculated by this law are shown in fig. 12.

It can be seen that the agreement with the second order solution is excellent on heads 2 and 3 and on the front half of head 1; C_p appears to be overestimated on the rear half of head 1 by amounts varying from about 1% of C_{pN} at $x = 0.6$ to 3% at $x = 0.9$ and 9% at $x = 1$.

On head 4, the agreement is excellent as far as $x = 0.7$ at $M = 1.6$ and good as far as $x = 0.5$ at $M = 2.8$. Towards the end of the head the law fails to take account of the slight recompression and for $M = 1.6$ a large error results at $x = 1$.

5.6. Merits and Limitations of the Five Methods.

On the basis of the results presented in section 5.1 to 5.5, it appears that the methods which give the best agreement with van Dyke's second order theory are the step-by-step method and the ogive of curvature method, using L.A.t.024. There is little to choose between

the accuracy of these two methods. Since the latter method is the simpler and more rapid of the two, its use will be preferable in most cases. Once the distributions of θ and χ along the head have been determined, the time required to compute one pressure distribution by the ogive of curvature method, using L.A.t.024, is about $1\frac{1}{2}$ hours, as compared with about 3 hours by the step-by-step method.

The ogive of curvature method, using NACA TN.2250, allows a further saving in computing time (one pressure distribution can be computed in about 40 minutes) but, generally, results in slight loss of accuracy (see section 5.3).

The $\log p \sim \theta$ law is the most rapid of the five methods, as it requires only about 20 minutes to pressure plot a head shape. It gave very good agreement with van Dyke's theory in all the cases investigated, except near the end of head 4. It is suitable, as is also the somewhat less accurate derivative formula, for investigations in which C_p is required as an explicit function of head geometry and Mach number.

The choice of the most suitable method to use in a particular case does not depend solely on the accuracy which the methods can be expected to give and on the computing labour involved but also, to a certain extent, on the geometry of the head. If the radius of curvature becomes zero at some point (as, for example, on heads 1 and 3), the ogive of curvature method, using NACA TN 2250, ceases to give results when the radius of curvature becomes sufficiently small, as then K falls outside the range of fig 3, whilst the derivative formula incorrectly predicts perfect vacuum where the radius of curvature is zero. No serious difficulty is experienced in this case with the step-by-step method and the ogive of curvature method using L.A.t.024, since the pressure distribution can be calculated right up to the point of zero radius of curvature by assuming that $\lambda \rightarrow 1$ as $\rho \rightarrow 0$. This assumption is justified by the fact that for flow round a sharp corner the changes of pressure are two-dimensional, i.e. $\lambda = 1$ when $\rho = 0$. In practice, it is sufficient to assume in this case that along the usually small portion of the head where λ cannot be found from figs. 1 or 6, λ is constant and equal to the arithmetic mean of 1 and

the last value of λ that can be determined. With the ogive of curvature method using L.A.t.024, the step-by-step method is used in the small region of large curvature where Fig. 1 cannot be used. This procedure was adopted in calculating the pressure distributions for $0.9 \leq x \leq 1$ on heads 1 and 3 and, as can be seen from figs 8a and 9a, resulted in very good agreement with the second order solutions. Almost equally good agreement was obtained there with the $\log p \sim \theta$ law (fig 12a). This law has the additional advantage that it requires no special treatment as $p \rightarrow 0$. Thus, when the radius of curvature tends to zero at some point on the head, the suitable methods to use are the ogive of curvature method (using L.A.t.024), the step-by-step method and the $\log p \sim \theta$ law.

On heads whose radius of curvature becomes infinite at the point of zero slope (as, for example, on heads 4 and 5), the step-by-step method and the ogive of curvature methods cannot predict pressure distributions over the last 5 - 20% of the head length, depending on Mach number and head geometry. The derivative formula and the $\log p \sim \theta$ law give values of C_p over the entire head length but, as the calculated distributions on head 4 seem to indicate (figs 11b and 12b), they become unreliable as the end of the head is approached. On this head the best overall accuracy was obtained with the two ogive of curvature methods. Over the rear end of the head, the ogive of curvature method using NACA TN.2250 is able to predict, with reasonable accuracy, the small recompression that takes place there (see fig. 10b); the same method using L.A.t.024 is not so satisfactory in this respect, but is more accurate over the forward 60% of the head. With these two methods, the errors in C_p along the rear of the head amount to about 7% of C_{pN} and are greater than in the case of heads terminating with a finite or zero radius of curvature.

Fig. 13 shows pressure distributions calculated for head 5 at $M = 2.0$ by the five methods. On this head, too, p becomes infinite at the point of zero slope and here again it is evident that over the first 40% of the head length the agreement between the different methods is very good, but as the end of the head is approached, the

methods begin to diverge. At $x = 0.6$, the difference between the extreme values of C_p is only about 3% of C_{pN} , increasing to about 7½% at $x = 0.8$. It thus appears that the inaccuracies in the pressure distributions predicted over the rear end of heads 4 and 5 are associated with the radius of curvature becoming infinite at the point of zero slope. It should be emphasized that in this case, though the predicted pressures are not very accurate near the end of the head, this is of little consequence in calculating the wave drags for between $x = 0.8$ and 1 the slope is very small (c.f. fig. 7 heads 4 and 5) and the contribution of this part of the head to the wave drag of the head is also very small, so that even relatively large errors in C_p have negligible effect on drag.

On the basis of the results obtained in only three cases, viz. head 4 at $M = 1.6$ and 2.8 and head 5 at $M = 2.0$, the best working rule for heads with infinite radius of curvature at the point of zero slope, $x = 1$, is probably as follows: Determine the pressure distribution by the ogive of curvature method using L.A.t.024 up to $x = 0.7$, then from $x = 0.7$ to 0.9 (or as close to 0.9 as possible) by the ogive of curvature method using NACA TN.2250, and from $x = 0.9$ to 1.0 take the pressure to remain constant at its value at $x = 0.9$. Around $x = 0.7$, fair in by eye the two arcs of curve.

Another point that arises in connection with head 4 is the apparent discrepancy between all the pressure distributions calculated by the methods of this report on head 4 at $M = 1.6$, and the corresponding second order pressure distributions over the rear half of the head. As was seen from figs 8b to 12b, this discrepancy begins at about $x = 0.4$, but up to $x = 0.7$ the five methods agree well with each other. It seems unlikely that this is purely the effect of the head shape, since results for head 4 at $M = 2.8$ and head 5 indicate that when the geometry of the heads causes inaccuracies in the present methods, there are discrepancies not only between the predicted and the second order pressure distributions, but also between the pressure distributions predicted by the five methods. It is believed that these discrepancies on head 4 at $M = 1.6$ can be accounted for, at least partly, by the

possible slight inaccuracy of the second order solution, In this solution, the boundary condition is satisfied at a number of control points along the body and for the same accuracy the number of points should be increased with decreasing Mach number (roughly, in proportion to $\sqrt{M^2 - 1}$). To save time and computing labour the number of control points on head 4 at $M = 1.6$ was kept the same as on other heads at $M = 2.0$ and head 4 at $M = 2.8$ and, consequently, this solution is likely to be less accurate than the others.

The recommended methods to use in any particular case are given in the following table:

Type of Head Shape	Method Giving Best Combination of Accuracy and Speed.	Method Giving Greatest Accuracy.
Radius of curvature everywhere finite and nowhere zero.	Either Log $p \sim \theta$ law; or ogive of curvature method using L.A.t.024.	Step-by-Step Method.
Radius of curvature zero at some point on the profile.	Ogive of Curvature Method, using L.A.t.024 (ref 4); Step-by-step method is used in the small region of large curvature where fig. 1. cannot be used.	Step-by-Step Method.
Radius of curvature infinite at the point of zero slope on the profile, $x = 1$.	$0 \leq x \leq 0.7$; Ogive of curvature method, using L.A.t.024. $0.7 \leq x \leq 0.9$ (or as close to 0.9 as possible); Ogive of curvature method, using NACA TN. 2250. $0.9 \leq x \leq 1.0$; take pressure as remaining constant at its $x = 0.9$ value. Around $x = 0.7$ fair in the two curves by eye.	

TABLE I

From Figs. 8 - 13 the accuracy which the recommended methods can be expected to give is as follows:-

for heads with:-

- (i) radius of curvature nowhere infinite (but can be zero at some point on the profile) - all the cases investigated here indicate that accuracy better than $\pm 2\%$ of C_{PN} can be obtained over the whole of the head length;
- (ii) radius of curvature infinite at the point of zero slope on the

profile - accuracy of C_p within 4% of C_{pN} should be obtainable within the range of figs 1 and 3. This conclusion is arrived at disregarding the results for head 4 at $M = 1.6$, since the accuracy of the corresponding second order solution is believed to be inferior to that of the other second order solutions.

On all the head shapes which were pressure plotted, y and all its derivatives with respect to x are everywhere continuous. However it is only necessary that y and its first three derivatives be continuous. For consider a head along which one of the higher derivatives of y , say y_4 , is discontinuous at some point D. Then since p depends on θ and X (by the basic assumption of the ogive of curvature method) i.e. depends on y, y_1 and y_2 , p and $\frac{dp}{dx}$ are continuous at D. Now at some point E on the head, at a sufficient distance downstream of the discontinuity at D the pressure distribution is uninfluenced by conditions at D, which is far upstream, and the method of this report will give the pressures correctly. So the methods of this report give correctly both p and $\frac{dp}{dx}$ at D and E. i.e. give correctly both ordinate and tangent of the ($p \sim x$) curve at D and E. Moreover the curve of p vs x derived from these methods is quite "smooth" between D and E (since p and $\frac{dp}{dx}$ are continuous), as also is the curve of exact, inviscid p vs x (since p and $\frac{dp}{dx}$ are continuous). Hence between D and E the exact curve of p and the curve of p by the methods of this report cannot depart from each other to any appreciable extent. Hence the methods of this report may be taken to apply accurately provided y and its first three derivatives with respect to x are continuous.

§6. Conclusions.

- Five different methods of pressure plotting an arbitrary pointed, convex, axi-symmetric head shape have been developed. All the methods give very good or good agreement with accurate pressure distribution, at $M = 1.6, 2.0$ and 2.8 obtained by applying van Dyke's second order theory of refs. 1 and 2, on four head shapes with convex, concave, convex-concave and concave-convex slope distributions. Worked examples of the application

of three of the five methods are given in Appendices I and II.

2. The five methods are also known to give with good accuracy the pressure distributions on circular arc ogives and to give cone pressures either exactly or with good accuracy; i.e. the methods apply too to heads with linearly varying and constant slope distributions. The methods can thus be applied for predicting pressures on pointed convex head shapes with any slope distribution likely to occur in practice, provided the ordinate and its first three derivatives are continuous along the head.

3. The quickest and slowest of these methods take about 20 minutes and 3 hours respectively to pressure plot an arbitrary head shape with given geometric details. When these methods are used, there is a very large saving of time without loss of accuracy compared with the time required when using the method of characteristics or van Dyke's second order theory, which both laboriously trace the flow step-by-step from the nose and require several days for the computations.

4. The best method out of the five to use for any particular head shape depends on the behaviour of the radius of curvature along the profile and on the accuracy and speed required. Recommended methods are listed in Table I of 5.6.

5. When the recommended methods are used, for the cases for which pressure distributions are given in this report C_p is predicted to within $\pm 2\%$ of C_{pN} if the radius of curvature nowhere tends to infinity, and to within $\pm 4\%$ of C_{pN} if and near where the radius of curvature tends to infinity at the point of zero slope. It is considered that the same accuracy will be obtained, using the recommended methods, on any pointed convex head shape for which the ordinate and its first ^{three} derivatives are continuous, so long as the effects of rotation produced by the curved shock wave are negligible. (Sec 2.6).

6. Two of these methods give C_p as a function of the radius y , $\frac{dy}{dx}$ and $\frac{d^2y}{dx^2}$, and may be used to determine minimum drag head shapes by applying the calculus of variations. The application of these two methods to this problem will be described in a later report.

7. The results of this report indicate that the pressure on a

pointed body of revolution at a point P depends solely on the local geometry at P and is independent of conditions upstream of P.

8. The methods of this report are of direct application in obtaining accurate values of lift, pressure, moment, etc. of a body at incidence by the hybrid procedure proposed by van Dyke in ref. 1.

9. It may be possible to adapt the methods of this report to give the external pressures on ducted bodies of revolution with attached external shock. A possible approach is suggested.

References.

<u>No.</u>	<u>Title.</u>	<u>Author</u>	<u>Identification.</u>
1.	First and Second Order Theory of Supersonic Flow Past Bodies of Revolution.	van Dyke, M.D.	J. Ae. Sci. March, 1951.
2.	A Study of Second-Order Supersonic Flow Theory.	van Dyke, M.D.	NACA T.N.2200.
3.	Resistance of Slender Bodies Moving with Supersonic Velocities, with Special Reference to Projectiles.	von Karman, T. Moore, N.B.	Trans A.S.M.E. Vol. 54, No.23 Dec. 15, 1932. p.p. 303-310.
4.	A Method for Calculating Pressure Distributions on Circular Arc Ogives at Zero Incidence at Supersonic Speeds, Using the Prantl-Meyer Flow Relations.	Zienkiewicz, H.K.	English Electric Co. Rept. L.A.t. 024, also ARC 14,790, FM 1702.
5.	Tables of Supersonic Flow Around Cones.	Kopal, Z.	M.I.T. Tech. Rept. No.1.
6.	An Analysis of the Applicability of the Hypersonic Similarity Law to the Study of Flow About Bodies of Revolution at Zero Angle of Attack.	Ehret, Dorris, M. Rossow, V.J. Stevens, V.I.	NACA. TN. 2250.
7.	Elements of Aerodynamics of Supersonic Flows.	Ferri, A.	Published by The Macmillan Co. New York.
8.	Computation Curves for Compressible Fluid Problems.	Dailey, C.L. Wood, F.C.	Published by: John Wiley and Sons, Inc.
9.	Supersonic Flow past Bodies of Revolution.	Lighthill, M.J.	R & M 2003
10.	Applicability of the Hypersonic Similarity Rule to Pressure Distributions which include the Effects of Rotation for Bodies of Revolution at Zero Angle of Attack.	Rossow, V.J.	NACA TN. 2399.

Appendix IThe Numerical Application of the λ Step-by-Step Method to a Non-Circular Profile.

In fig 5, Q is a point on the profile a short distance from P. Knowing the static pressure at P, it is required to find it at Q.

SAP is the circle of curvature at P to the profile and A is its intersection with the axis of the body. S is the sonic point of the Prandtl-Meyer expansion introduced when applying the method of ref. 4 to expansion round the circular arc ogive AP. We shall first determine the position of S, by determining v_A so that it gives the correct static pressure at P on the circular arc ogive SAP.

Let $F(v)$ denote the ratio of static to stagnation pressure after Prandtl-Meyer expansion through an angle v from sonic velocity. $F(v)$ is given in Table I of ref. 7. Then by the theory of ref. 4,

$$\left(\frac{p}{p_{stag_A}}\right) = F(v_A) \quad \dots \dots \dots (i)$$

$$\text{and} \left(\frac{p}{p_{stag_A}}\right) - \left(\frac{p}{p_{stag_P}}\right) = \lambda \left[F(v_A) - F(v_P) \right]$$

$$F(v_A) - \left(\frac{p}{p_{stag_P}}\right) = \lambda \left[F(v_A) - F(v_P) \right]$$

$$F(v_A) - \left(\frac{p}{p_{stag_P}}\right) = \lambda \left[F(v_A) - F(v_A + \phi) \right] \quad \dots \dots \dots (ii)$$

where ϕ is the angle, $(\chi_P - \theta_P)$, between the tangents at A and P to the circle of curvature at P.

In equation (ii), v_A and λ are the unknowns, ϕ and $\left(\frac{p}{p_{stag_P}}\right)$ are known.

Now λ is a function of circular arc ogive geometry and free stream Mach number \bar{M} ; thus λ is a function of χ_P and of $\left(\frac{p}{p_{stag_A}}\right)$, for these second two quantities uniquely determine the first two quantities. Therefore, by virtue of equation (i), λ is a function of χ_P and v_A . In Fig. 6, λ is plotted against χ_P and v_A and this chart connecting λ and v_A together with equation (ii) uniquely determines λ and v_A for given $\left(\frac{p}{p_{stag_P}}\right)$, ϕ and χ_P . Lines

of constant \bar{M} are also shown in Fig.6.

To solve for λ and v_A , let:

$$\left(\frac{p}{p_{stag}}\right)_P = F(\omega). \quad \text{Then } \omega \text{ is known}$$

since $\left(\frac{p}{p_{stag}}\right)_P$ is known.

Equation (ii) becomes:

$$\lambda = \frac{F(v_A) - F(\omega)}{F(v_A) - F(v_A + \phi)} \quad \dots \dots \dots (iii)$$

i.e. $\lambda = G(v_A)$ since ω and ϕ are known.

Now $G(\omega - \phi) = 1$ and $G(\omega) = 0$. Therefore, since λ is generally between 1.0 and 0.75, and usually closer to 0.75 than to 1.0 we can take $v_A = (\omega - \phi)$ and $v_A = (\omega - \frac{3}{4}\phi)$ as first and second approximations to v_A . These values of v_A will give corresponding pairs of values of λ , viz. λ_1 from equation (iii) and λ_2 from Fig. 6. At the correct value of v_A , λ_1 and λ_2 are equal. By calculating the differences $\Delta \lambda = (\lambda_1 - \lambda_2)$ we can interpolate linearly to obtain the value of v_A corresponding to $\Delta \lambda = 0$. In nearly all cases it is sufficiently accurate to take the first interpolated value of v_A as the correct v_A . λ and \bar{M} (if required) are then read from Fig.6 at this value of v_A and the particular value of X_P . When this procedure is systematised on a proforma only a few minutes are required to find v_A , λ and \bar{M} .

With these three quantities known, the pressure at Q is readily determined. By the fundamental assumption, the flow expands from P to Q (Fig. 5) as if the body were replaced between P and Q by the ogive of curvature at P. Therefore the pressure at Q is given by:

$$\left(\frac{p}{p_{stag}}\right)_P - \left(\frac{p}{p_{stag}}\right)_Q = \lambda [F(v_P) - F(v_Q)]$$

$$\text{i.e. } \left(\frac{p}{p_{stag}}\right)_Q = \left(\frac{p}{p_{stag}}\right)_P - \lambda [F(v_A + X_P - \theta_P) - F(v_A + X_P - \theta_Q)] \dots \dots (iv)$$

All the quantities on the right hand side are known; hence $\left(\frac{p}{p_{stag}}\right)_Q$ and hence C_p at Q.

Some Practical Points.

The best way to space the points at which the pressures are determined is so that θ varies by roughly equal amounts between successive points, unless and except where χ varies very rapidly and here finer intervals should be taken. (For λ will vary very rapidly, too).

As the solution proceeds λ should be plotted against x and by extrapolating this curve the mean value of λ over the next interval can be quite accurately predicted. This mean value, and not the value of λ at the start of the interval, should be used in equation (iv) to eliminate the small error introduced by taking finite steps instead of infinitesimal ones.

If required, a second approximation can be obtained, using the curve of λ obtained in the first approximation as a guide when extrapolating to find the mean λ 's. In practice, a second approximation is unnecessary unless the head shape has very rapid curvature at some point.

It will be found a considerable help to plot on a generous scale (i) $F(\nu)$ vs, ν , as given in Table I of ref. 7, and (ii) cone C_p vs θ_s for various convenient values of M , as given in ref. 5.

Numerical Example of the λ Step-by-Step Method.

$$\text{Profile: } y = \frac{1}{6} [1 - (1 - 0.6x)^3]; \quad 0 \leq x \leq 1.0$$

$$\frac{L}{D} = 3.205; \quad \theta_s = \tan^{-1} 0.3 = 16.70^\circ$$

$$M = 2.0$$

Divide the head into 5 intervals so that θ changes by roughly the same amount in each interval, with finer intervals only if and where χ varies very rapidly.

$$\theta = \tan^{-1} y_1 = y_1$$

$$\chi = \cos^{-1} \left\{ \frac{(1 + y_1^2 + y_2^2) - (1 + y_1^2 + y_2^2)}{(1 + y_1^2)^{3/2}} \right\} = \sqrt{y_1^2 - 2y_1y_2}$$

A quick check on the values of $\sqrt{y_1^2 - 2y_1y_2}$ and y_1 shows that χ varies slowly over the entire head and that for approximately equal increments of θ the limits of the intervals should be as follows:

$$x = 0, 0.1, 0.3, 0.5, 0.7 \text{ and } 1.0.$$

χ , θ and $\phi (= \chi - \theta)$ are required at these points. y , y_1 and y_2 are given by:

$$y = \frac{1}{6} \left\{ 1 - (1 - 0.6x)^3 \right\}$$

$$y_1 = 0.3 (1 - 0.6 x)^2$$

$$y_2 = -0.36 (1 - 0.6x)$$

Hence, using the exact formulae for θ and χ :

x	0	0.1	0.3	0.5	0.7	1.0
θ (DEG)	16.70	14.85	11.40	8.37	5.77	2.75
χ (DEG)	16.70	16.67	16.33	15.77	14.67	12.42
ϕ (DEG)	0	1.82	4.93	7.40	8.90	9.67

TABLE II

First Interval. $0 \leq x \leq 0.1$

For the first interval, λ is taken as the value corresponding to the nose semi-angle of the head, 16.7° , and the free stream Mach number 2.0.

$$\lambda = 0.793, \text{ from Fig.1.}$$

The starting point of the solution is $C_p = 0.241$ just behind the nose shock (From ref.5).

$$\text{From Table I, ref. 7, } \frac{P_{stag_0}}{P_0} = 7.82 \text{ at } M = 2.0$$

From ref, 8 fig 3-2,

stagnation pressure ratio across nose shock, at nose = 0.996.

$$\text{At the first point (x = 0), } \frac{P}{P_{stag}} = \frac{1 + 0.241 \times 2.8}{0.996 \times 7.82} = 0.214$$

For the first interval, A coincides with N (see Fig.5).

$$\text{From equation (i), } F(v_A) = 0.214, \text{ so } v_A = 16.72^\circ \text{ (Table I, ref. 7)}$$

From Table II,

$$\chi_p - \theta_p = 16.7^\circ - 16.7^\circ = 0; \quad \chi_p - \theta_Q = 16.7^\circ - 14.85^\circ = 1.85^\circ$$

$$v_A + \chi_p - \theta_p = 16.72^\circ, \quad v_A + \chi_p - \theta_Q = 16.72^\circ + 1.85^\circ = 18.57^\circ$$

$$\therefore F(v_A + \chi_p - \theta_p) = 0.2140 \text{ and } F(v_A + \chi_p - \theta_Q) = 0.1948$$

$$\text{Now } \left(\frac{P}{P_{stag}} \right)_P = 0.214 \text{ and } \lambda = 0.793.$$

$$\left(\frac{P}{P_{stag}} \right)_Q = 0.214 - 0.793 \left\{ 0.2140 - 0.1948 \right\} \text{ by equation (iv)}$$

$$= 0.1988, \text{ at } x = 0.1$$

2nd Interval. $0.1 \leq x \leq 0.3$

First find λ . $F(\omega) = \left(\frac{p}{p \text{ stag}} \right)_{x=0.1} = 0.1988$; $\omega = 18.18^\circ$ (Table I, refer. 7).

From Table II, at $x = 0.1$, $\phi = 1.82^\circ$ and $\chi_p = 16.67^\circ$ $\omega - \phi = 16.36^\circ$, $\omega - \frac{3}{4}\phi = 16.81^\circ$. (These are the first and second approximations to ν_A .)

(1) Assumed ν_A (DEG.)	(2) $F(\nu_A) = F(1)$ (Table I, ref. 7).	(3) $\nu_A + \phi$ = (1) + 1.82° (DEG.)	(4) $F(\nu_A + \phi)$ = $F(3)$ (Table I, ref. 7).	(5) $F(\nu_A) - F(\omega)$ = (2) - 0.1988	(6) $F(\nu_A) -$ $F(\nu_A + \phi)$ = (2) - (4)	(7) $\lambda_1 = \frac{(5)}{(6)}$	(8) λ_2 from Fig. 6 at (1) and $\chi_p = 16.67^\circ$	(9) $\Delta \lambda = \lambda_1 - \lambda_2$ = (7) - (8)
$\omega - \phi = 16.36$	/	/	/	/	/	1.0	0.790	0.210
$\omega - \frac{3}{4}\phi =$ 16.81	0.2130	18.63	0.1940	0.0142	0.0190	0.747	0.794	-0.047
By inter- polation, 16.73	0.2140	18.55	0.1950	0.0152	0.190	0.800	0.793	0.007

The agreement in columns (7) and (8) is sufficiently good at this stage. (A further interpolation only gives $\nu_A = 16.74^\circ$ and $\lambda = 0.793$). Hence from columns (1) and (8), $\nu_A = 16.73^\circ$, $\lambda = 0.793$. Also, from Fig. 6 at $\nu_A = 16.73^\circ$ and $\chi_p = 16.67^\circ$, $M = 2.0$.

From Table II, $\chi_p - \theta_p = 16.67^\circ - 14.85^\circ = 1.82^\circ$; $\chi_p - \theta_Q = 16.67^\circ - 11.40^\circ = 5.27^\circ$
 $\nu_A + \chi_p - \theta_p = 16.73^\circ + 1.82^\circ = 18.55^\circ$; $\nu_A + \chi_p - \theta_Q = 16.73^\circ + 5.27^\circ = 22.0^\circ$
 $F(\nu_A + \chi_p - \theta_p) = 0.1950$, $F(\nu_A + \chi_p - \theta_Q) = 0.1625$; $\left(\frac{p}{p \text{ stag}} \right)_p = 0.1988$; $\lambda = 0.793$

$\left(\frac{p}{p \text{ stag}} \right)_Q = 0.1988 - 0.793 (0.1950 - 0.1625) = 0.1730$, at $x = 0.3$

3rd Interval. $0.3 < x \leq 0.5$

$$F(\omega) = 0.1730; \omega = 20.8^\circ; \phi = 4.93^\circ; (\omega - \phi) = 15.87^\circ; (\omega - \frac{3}{4}\phi) = 17.1^\circ; X_p = 16.33^\circ$$

(1) ν_A	(2) $F((1))$	(3) $(1) + 4.93^\circ$	(4) $F((3))$	(5) $(2) - 0.1730$	(6) $(2) - (4)$	(7) $\lambda_1 = \frac{(5)}{(6)}$	(8) λ_2 at (1) and $X_p = 16.33^\circ$	(9) $\Delta \lambda = (7) - (8)$
15.87	—	—	—	—	—	1.0	0.780	0.220
17.10	0.2100	22.03	0.1620	0.0370	0.0480	0.770	0.788	-0.018
17.01							0.788	

Further approximation is unnecessary and $\nu_A = 17.01^\circ$, $\lambda = 0.788$, $\bar{M} = 2.0$.

Extropolating λ to $x = 0.5$ gives mean $\lambda = 0.784$ for $0.3 \leq x \leq 0.5$.

$$X_p - \theta_p = 4.93^\circ, X_p - \theta_Q = 7.96^\circ; \nu_A + X_p - \theta_p = 21.94^\circ, \nu_A + X_p - \theta_Q = 24.97^\circ.$$

$$F(\nu_A + X_p - \theta_p) = 0.1629; \quad F(\nu_A + X_p - \theta_Q) = 0.1382.$$

$$\therefore \left(\frac{P}{P_{stag/Q}} \right) = 0.1730 - 0.784 (0.1629 - 0.1382) = 0.1536, \text{ at } x = 0.5$$

4th Interval. $0.5 \leq x \leq 0.7$.

$$F(\omega) = 0.1536; \omega = 23.04^\circ \quad \phi = 7.40^\circ \quad (\omega - \phi) = 15.64^\circ; \quad (\omega - \frac{3}{4}\phi) = 17.49^\circ. \quad \chi_p = 15.77^\circ.$$

(1) ν_A	(2) $F(1)$	(3) $(1) + 7.40^\circ$	(4) $F(3)$	(5) $(2) - 0.1536$	(6) $(2) - (4)$	(7) (5) $\lambda_1 = \frac{\quad}{(6)}$	(8) λ_2 at (1) at $\chi_p =$ 15.77°	(9) $\Delta\lambda = (7) - (8)$
15.64	/	/	/	/	/	1.0	0.769	0.231
17.49	0.2058	24.89	0.1389	0.0522	0.0669	0.781	0.782	-0.001

Hence $\nu_A = 17.49^\circ$, $\lambda = 0.782$, $\bar{M} = 2.0$. Extrapolating λ to $x = 0.7$, gives mean $\lambda = 0.777$ for $0.5 \leq x \leq 0.7$.

$$\chi_p - \theta_p = 7.40^\circ; \quad \chi_p - \theta_Q = 10.0^\circ; \quad \nu_A + \chi_p - \theta_p = 24.89^\circ; \quad \nu_A + \chi_p - \theta_Q = 27.49^\circ.$$

$$F(\nu_A + \chi_p - \theta_p) = 0.1389; \quad F(\nu_A + \chi_p - \theta_Q) = 0.120$$

$$\therefore \left(\frac{P}{P \text{ stag } Q} \right) = 0.1536 - 0.777 (0.1389 - 0.1200) = 0.1389, \quad \text{at } x = 0.7.$$

5th Interval. $0.7 \leq x \leq 1.0$

$$F(\omega) = 0.1389; \omega = 24.89^\circ. \quad \phi = 8.90^\circ \quad (\omega - \phi) = 15.99^\circ; \quad (\omega - \frac{3}{2}\phi) = 18.22^\circ; \quad \chi_p = 14.67^\circ$$

(1) ν_A	(2) $F(1)$	(3) $(1) + 8.90^\circ$	(4) $F(3)$	(5) $(2) - 0.1389$	(6) $(2) - (4)$	(7) $\lambda_1 = \frac{(5)}{(6)}$	(8) λ_2 at $\chi_p = 14.67^\circ$	(9) $\Delta \lambda = \frac{(7) - (8)}{(8)}$
15.99	—	—	—	—	—	1.0	0.754	0.246
18.22	0.1980	27.12	0.1224	0.0591	0.0756	0.781	0.769	0.012
18.33							0.770	

Hence $\nu_A = 18.33, \lambda = 0.770, \bar{M} = 2.0$. Extrapolating λ to $x = 1.0$ gives mean $\lambda = 0.757$ for $0.7 \leq x \leq 1.0$.

$$\chi_p - e_p = 8.90^\circ; \chi_p - e_Q = 11.92^\circ; \nu_A + \chi_p - e_p = 27.23^\circ; \nu_A + \chi_p - e_Q = 30.25^\circ$$

$$F(\nu_A + \chi_p - e_p) = 0.1217; \quad F(\nu_A + \chi_p - e_Q) = 0.1020$$

$$\left(\frac{p}{p \text{ stags } Q} \right) = 0.1389 - 0.757 (0.1217 - 0.1020) = 0.1240, \text{ at } x = 1.0$$

C_p is found thus:

$$2.8 C_p + 1 = \frac{p}{P_0} = \frac{p}{P_{stag}} \times \frac{P_{stag}}{P_{stag_0}} \times \frac{P_{stag_0}}{P_0}$$

$$\frac{P_{stag}}{P_{stag_0}} = 0.996 \quad (\text{from Fig. 3-2, ref. 8})$$

$$\frac{P_{stag_0}}{P_0} = 7.82 \quad (\text{from Table I, ref. 7})$$

$$C_p = \frac{7.79 \frac{p}{P_{stag}} - 1}{2.8}$$

Hence the following values of C_p :

x	$\frac{p}{P_{stag}}$	C_p
0	0.214	0.241
0.1	0.1988	0.196
0.3	0.1730	0.124
0.5	0.1536	0.073
0.7	0.1389	0.029
1.0	0.1240	-0.012

These values of C_p are plotted in Fig. 8 (a).

A specimen proforma, for use with the λ step-by-step method, is given on the next page.

$F(\omega) =$; $\omega =$; $\phi =$; $(\omega - \phi) =$; $\frac{3}{4}\phi =$; $(\omega - \frac{3}{4}\phi) =$; $\lambda_p =$

①	②	③	④	⑤	⑥	⑦	⑧	⑨
v_A	$F(②)$	$① + \phi =$ $① +$	$F(③)$	$② - F(\omega) =$ $② -$	$② - ④$	$\lambda_1 = \frac{⑤}{⑥}$	λ_2 at ① and $\lambda_p =$ from fig.	$\Delta\lambda = ⑦ - ⑧$
$(\omega - \phi) =$	/	/	/	/	/	1.0		
$(\omega - \frac{3}{4}\phi) =$								

Hence $v_A =$, $\lambda =$, $\bar{M} =$. Extrapolating λ to $x =$ gives mean $\lambda =$ for $\leq x \leq$

$X_p - \theta_p =$; $X_p - \theta_Q =$; $v_A + X_p - \theta_p =$; $v_A + X_p - \theta_Q =$
 $F(v_A + X_p - \theta_p) =$; $F(v_A + X_p - \theta_Q) =$

$\left(\frac{P}{P_{stag}}\right)_Q = F(\omega) - \lambda_{mean} (F[v_A + X_p - \theta_p] - F[v_A + X_p - \theta_Q])$

APPENDIX IIExample of the Application of the Ogive of Curvature Method.

$$\text{Profile: } y = \frac{1}{8} \left\{ 1 - (1 - x)^3 \right\}; \quad 0 \leq x \leq 1.0$$

$$\frac{L}{D} = 4.0; \quad \theta_s = \tan^{-1} \frac{3}{8} = 20.55^\circ$$

$$M = 2.0$$

We shall find the pressures at the points $x = 0, 0.2, 0.4, 0.6, 0.8$ and 1.0 . The values of:

$$\theta = \tan^{-1} y_1$$

$$X = \cos^{-1} \left\{ \frac{1 + y_1^2 + y_1 y_2}{(1 + y_1^2)^{\frac{3}{2}}} \right\}$$

$$\left(X - \theta \right)$$

$$\left(1 - \frac{\theta}{X} \right)$$

are required. They are given in the table below:

x	θ (DEG)	X (DEG)	$(X - \theta)$ (DEG)	$1 - \frac{\theta}{X}$
0	20.55	20.55	0	0
0.2	13.50	20.15	6.65	0.330
0.4	7.68	18.53	10.85	0.585
0.6	3.43	15.87	12.44	0.785
0.8	0.85	11.10	10.25	0.923
1.0	0	0	0	0

TABLE III

We can calculate pressures on the body using the methods of either ref.4 or ref.6. In both cases we make the assumption that the ratio of static to stagnation pressure at P on a body at free stream Mach number M is equal to this ratio at P on the ogive of curvature at P at the same free stream Mach number M. We proceed as follows:

(a) By the Method of L.A.t.02 (ref.4)

After determining $\frac{p}{p_{\text{stag}}}$ at the nose of the ogive of curvature, the decrease in $\frac{p}{p_{\text{stag}}}$ from this value to its value at the point concerned is

determined as a fraction, λ , of the two-dimensional decrease in $\frac{p}{p_{stag}}$ over the same profile.

Having determined $\frac{p}{p_{stag}}$ along the head, C_p is found thus:

$$\frac{p_{stag_0}}{p_0} = 7.82 \text{ (Table I, ref. 7)}; \frac{p_{stag}}{p_{stag_0}} = 0.989 \text{ (fig. 3-2, ref. 8)}$$

$$2.8 C_p + 1 = \frac{p}{p_0} = 7.74 \frac{p}{p_{stag}}; \text{ i.e. } C_p = 2.76 \frac{p}{p_{stag}} - 0.357$$

(1) α	0	0.2	0.4	0.6	0.8	1.0
(2) χ from Table III	20.55	20.15	18.53	15.87	11.1	0
(3) C_p at (2) and $M = 2$ (Ref. 5).	0.340	0.3295	0.286	0.2215	0.1237	
(4) $1 + 2.8 \times (3)$ $= \frac{P_A}{P_0}$		1.922	1.801	1.620	1.346	
(5) P_{stag_0} at $M = 2$ from P_0 Table I Ref. 7.		7.82	7.82	7.82	7.82	
(6) P_{stag} at (2) and $M=2$ (fig 3-2, $\frac{P_{stag_0}}{P_0}$ Ref. 3)		0.990	0.992	0.998	1.0	
(7) $5) \times (6) = \frac{P_{stag}}{P_0}$		7.74	7.76	7.80	7.82	
(8) $(4) \div (7) = \frac{P_A}{P_{stag}}$		0.2482	0.2320	0.2078	0.1720	
(9) V_A at (8), from Table I, ref. 7.		13.79	15.12	17.30	20.92	
(10) $(\chi - \epsilon)$ from Table III		6.65	10.85	12.44	10.25	
(11) $(9) + (10)$		20.44	25.97	29.74	31.17	
(12) $\frac{P}{P_{stag}}$ at (11) from Table I, Ref. 7.		0.1765	0.1306	0.1053	0.0966	
(13) $(8) - (12) =$ $(\Delta \frac{P}{P_{stag}})_{2-D}$		0.0717	0.1014	0.1025	0.0754	
(14) λ at (2) and $M=2$ from Fig. 1.		0.835	0.816	0.783	0.744	
(15) $(13) \times (14) =$ $(\Delta \frac{P}{P_{stag}})_{A-S}$		0.0599	0.0827	0.0803	0.0560	
(16) $(8) - (15) = \frac{P}{P_{stag}}$		0.1883	0.1493	0.1275	0.1160	
(17) $2.76 \times (16)$		0.520	0.412	0.352	0.320	
(18) $(17) - 0.357 = C_p$	0.340	0.163	0.055	-0.005	-0.037	-0.056 (Extrapolated)

As, at $M = 2$, λ is unavailable for values of χ less than 11° (See Fig. 1), the curve of C_p vs α is extrapolated (without difficulty) the short distance from $\alpha = 0.8$ to $\alpha = 1.0$.

The values of C_p in column (18) are plotted in Fig. 13.

(b) By the Method of NACA TN 2250 (Ref. 6)

At $M = 2$ the stagnation pressure loss is less than 1% across conical shocks produced by nose semi-angles of up to $20\frac{1}{2}^\circ$. Hence we can assume, with good accuracy, that if the surface stagnation pressures of the flows at $M = 2$ past the body and past the ogive of curvature are the same, then the corresponding free stream static pressures will be the same. (This will be exactly true at the nose of the body). Hence, since $\frac{p}{p_{stag}}$ is assumed the same for both body and ogive of curvature, the values of $\frac{p}{p_0}$ will be the same, too. $\frac{p}{p_0}$ on circular arc tangent ogives is shown in ref. 6 to depend solely on similarity parameter, K , and the per cent head length, P . For the ogive of curvature, these quantities are given by:

$$K = 2M \tan \frac{X}{2}$$

$$P = 100 \left(1 - \frac{\theta}{X} \right)$$

When K and P have been calculated, $\left\{ \frac{p}{p_0} - 1 \right\}$ is read from Fig. 3.

Hence follows C_p . The calculations are given in the following proforma:

(1) x	(2) X (DEG) from Table III	(3) $\frac{X}{2} \tan \frac{X}{4} = K$	(4) $P = 100(1 - \frac{\theta}{X})$ from Table III	(5) $P_{po} - 1$, from Fig. 3 at (3) and (4)	(6) $C_p = (5) - 2.8$
0	20.55	0.725	0	0.948	0.338
0.2	20.15	0.711	33	0.454	0.162
0.4	18.53	0.652	58.5	0.152	0.054
0.6	15.87	0.558	78.5	-0.015	-0.005
0.8	11.1	0.368	92.35	-0.082	-0.029
1.0	0	0			-0.019 (extra- polated)

To use Fig. 3, K must exceed 0.3. So the C_p vs. x curve was extrapolated from $x = 0.8$ to $x = 1.0$.

The above values of C_p are plotted in fig. 13.

APPENDIX III

Development of the Derivative Formula for Pressure on an
arbitrary Head.

In ref. 6, it is shown that on tangent circular arc ogives, the pressure is given by:

$$\frac{P}{P_0} = \left(\frac{P}{P_0} \right)_N 10^{-nx} \dots \dots \dots (i)$$

where x is distance along the head, x = 1 corresponding to the end of the tangent ogive. From Fig.10 of ref. 6, "Variation of the Logarithm of the Pressure Ratio along Ogives for Various Values of the Similarity Parameter," the following results were obtained:

(a) For values of similarity parameter K between 0.5 and 1.0, n is given by:

$$n = 0.61 K - 0.068 \dots \dots \dots (ii)$$

(b) For $0.4 \leq K \leq 1.0$, $\left(\frac{P}{P_0} \right)_N$ is given very closely by:

$$\log_{10} \left(\frac{P}{P_0} \right)_N = 0.485K - 0.062 \dots \dots \dots (iii)$$

Combining equations (i), (ii) and (iii) gives:

$$\log_{10} \left(\frac{P}{P_0} \right) = 0.485K - 0.062 - (0.61K - 0.068)x. \dots \dots \dots (iv)$$

Now x and K are given by:

$$x = 1 - \frac{\sin \theta}{\sin X}$$

$$K = 2M \tan \frac{X}{2}$$

where θ and X are the surface slope and nose semi-angle of the circular arc profile concerned.

For values of X up to 20° , the following approximate formulae involve not more than 1% error in the values of x and K:

$$\left. \begin{aligned} x &= 1 - \frac{\theta}{X} \\ K &= M X \end{aligned} \right\} \dots \dots \dots (v)$$

(In (v) θ and X are in radians).

Substitution of (v) in (iv) leads to:

$$\begin{aligned} \frac{P}{P_0} &= 10^{0.006 + 0.61M\theta - 0.125MX - 0.068 \frac{\theta}{X}} \\ &= 1.014 \times 10^{0.61M\theta - 0.125MX - 0.068 \frac{\theta}{X}} \\ \text{i.e. } \frac{P}{P_0} &= 1.014 e^{1.405M\theta - 0.288MX - 0.157 \frac{\theta}{X}} \dots \dots \dots (vi) \end{aligned}$$

As shown in Appendix II, provided the stagnation pressure losses of a body and the ogive of curvature at their nose shocks are both very small then $\frac{p}{p_0}$ will be effectively the same for both body and ogive of curvature. For $M \leq 2$, $\theta_s \leq 20^\circ$ the loss is $< 1\%$ and for $2 \leq M \leq 3$, $\theta_s \leq 15^\circ$ the loss is $< 2\%$. Hence for these ranges of M and θ_s equation (vi) gives the pressure on an arbitrary body, if θ and χ are taken as the surface slope of the body and nose angle of the ogive of curvature. θ and χ are then given by:

$$\theta = \tan^{-1} y_1 \quad \dots \dots \dots \text{(vii)}$$

$$\chi = \cos^{-1} \left[\cos \theta (1 + y y_2 \cos^2 \theta) \right]$$

where $y = y(x)$ is the profile of the body.

For $\theta \leq 17^\circ$, $\tan \theta$ differs from θ by not more than 3% so a good approximation to (vii) is:

$$\theta = y_1 \quad \dots \dots \dots \text{(viii)}$$

$$\text{Now } \cos \chi = \cos \theta (1 + y y_2 \cos^2 \theta)$$

$$\begin{aligned} \sin^2 \chi &= 1 - \cos^2 \chi = 1 - \cos^2 \theta (1 + y y_2 \cos^2 \theta)^2 \\ &= 1 - (1 - \sin^2 \theta) (1 + 2 y y_2 \cos^2 \theta + y^2 y_2^2 \cos^4 \theta) \end{aligned}$$

$$\text{i.e. } \sin^2 \chi = \left[\sin^2 \theta - 2 y y_2 \right] + \cos^2 \theta y y_2 (2 \sin^2 \theta - y y_2 \cos^4 \theta)$$

Denote by $\frac{L}{D}$ the fineness ratio of the ogive of curvature under consideration.

$$y y_2 = O \left(\frac{D^2}{L^2} \right)$$

$$\sin^2 \theta = O \left(\frac{D^2}{L^2} \right), \cos^2 \theta = O(1)$$

$$\chi = O \left(\frac{D}{L} \right)$$

$$\chi^2 + O \left(\frac{D^4}{L^4} \right) = \theta^2 - 2 y y_2 + O \left(\frac{D^4}{L^4} \right)$$

$$\chi^2 = y_1^2 - 2 y y_2 + O \left(\frac{D^4}{L^4} \right), \text{ by equation (viii)}$$

$$\text{i.e. } \chi^2 = (y_1^2 - 2 y y_2) \left(1 + O \left(\frac{D^2}{L^2} \right) \right)$$

So with a relative error of order only $\frac{D^2}{L^2}$, we have the approximate formula:

$$\chi = \sqrt{y_1^2 - 2 y y_2} \quad \dots \dots \dots \text{(ix)}$$

Substituting equations (viii) and (ix) in equation (vi) gives the

derivative formula for pressure on an arbitrary head, $y = y(x)$:

$$\frac{p}{p_0} = 1.014e^{1.405M y_1 - 0.288M \sqrt{y_1^2 - 2 y y_2} - 0.157 \sqrt{y_1^2 - 2 y y_2}}$$

APPENDIX IVThe Slope of the $\log p \sim \theta$ Curve at the Nose of a Body

For the purpose of determining pressure gradient at the nose, the profile of a body may be replaced by its circle of curvature at the nose, as pointed out in 2.1.

Therefore in Fig.2, at the nose, the decrease in pressure along an elementary length of profile is given by:

$$dp_{A-S} = \lambda_N dp_{2-D}, \text{ by the } \lambda \text{ - law for}$$

circular arc ogives of ref.4. (λ_N is the value of λ at the nose, corresponding to M and the nose angle θ_s of the profile).

$$\therefore \left(\frac{dp}{d\theta} \right)_{A-S} = \lambda_N \left(\frac{dp}{d\theta} \right)_{2-D} \quad \dots \quad \dots \quad \dots \quad (i)$$

Now in two-dimensional flow,

$$\left(\frac{dp}{d\theta} \right)_{2-D} = \frac{\gamma M_L^2 p}{\sqrt{M_L^2 - 1}} \quad \dots \quad \dots \quad \dots \quad (ii)$$

(where M_L is local Mach number).

Combining equations (i) and (ii), and remembering that the starting conditions, M_N and p_N , of the axi-symmetric and two-dimensional flows along the profile are the same, we obtain

$$\left(\frac{dp}{d\theta} \right)_{A-S} = \frac{\gamma \lambda_N M_N^2}{\sqrt{M_N^2 - 1}} p_N$$

$$\text{i.e.} \left[\frac{d(\log_e p)}{d\theta} \right]_{A-S} = \frac{\gamma \lambda_N M_N^2}{\sqrt{M_N^2 - 1}}, \text{ at the nose}$$

$$\text{But} \left[\frac{d(\log_{10} p)}{d\theta} \right]_{A-S} = \sigma$$

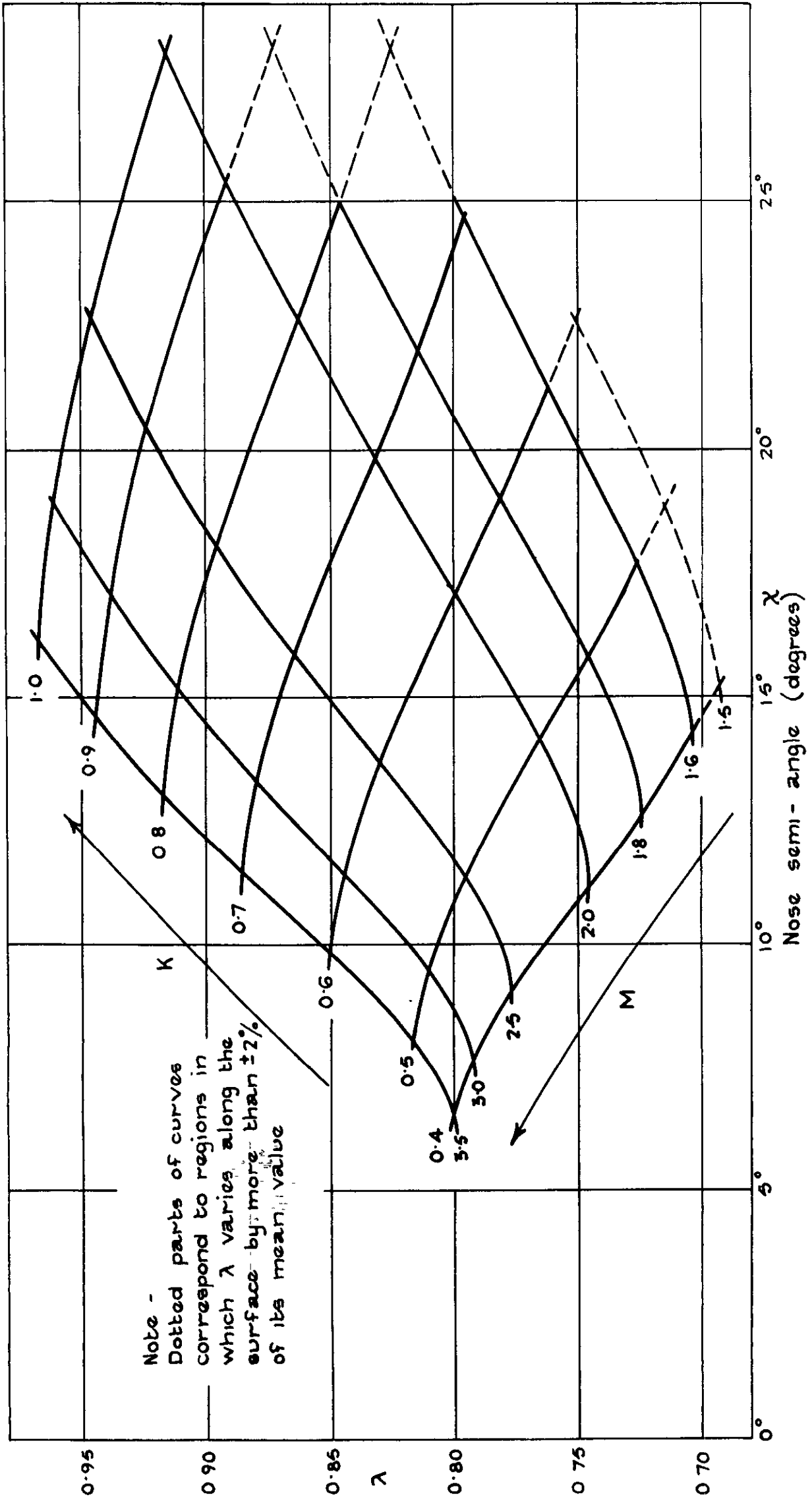
$$\sigma = \frac{0.4343 \gamma \lambda_N M_N^2}{\sqrt{M_N^2 - 1}}$$

In this formula, θ is measured in radians. If θ is measured in degrees and γ taken as 1.4, the formula becomes:

$$\sigma = 0.0106 \frac{\lambda_N M_N^2}{\sqrt{M_N^2 - 1}}$$

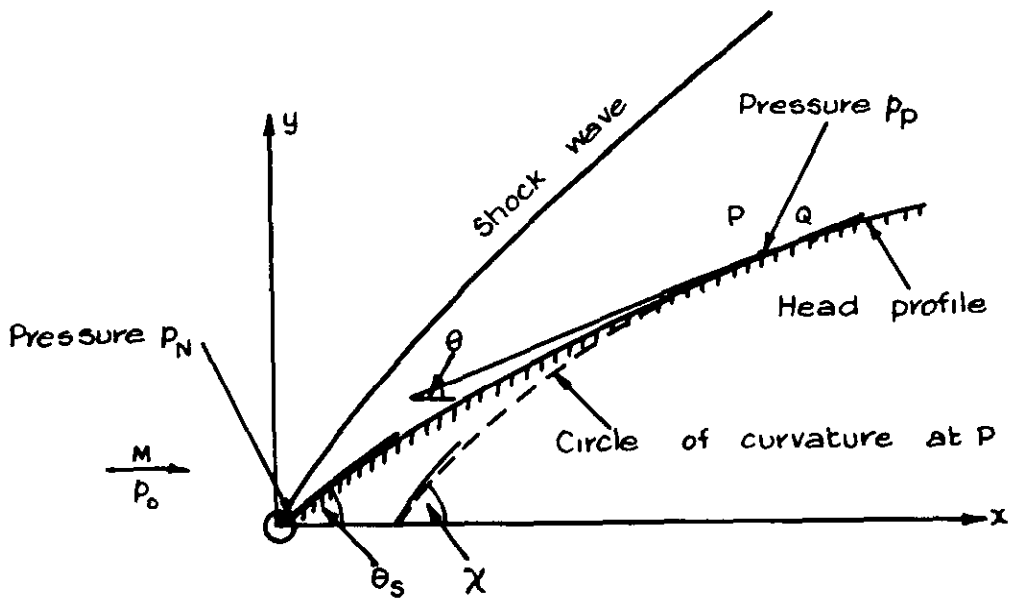
M_N and λ_N depend solely on the nose semi-angle θ_s of the body and free-stream Mach number M . In Fig. 4 σ , as given by this formula, is plotted against θ_s for various values of M .

FIG 1



Variation of λ with χ , M and K for circular arc ogives

FIG 2



Supersonic flow past an arbitrary headshape

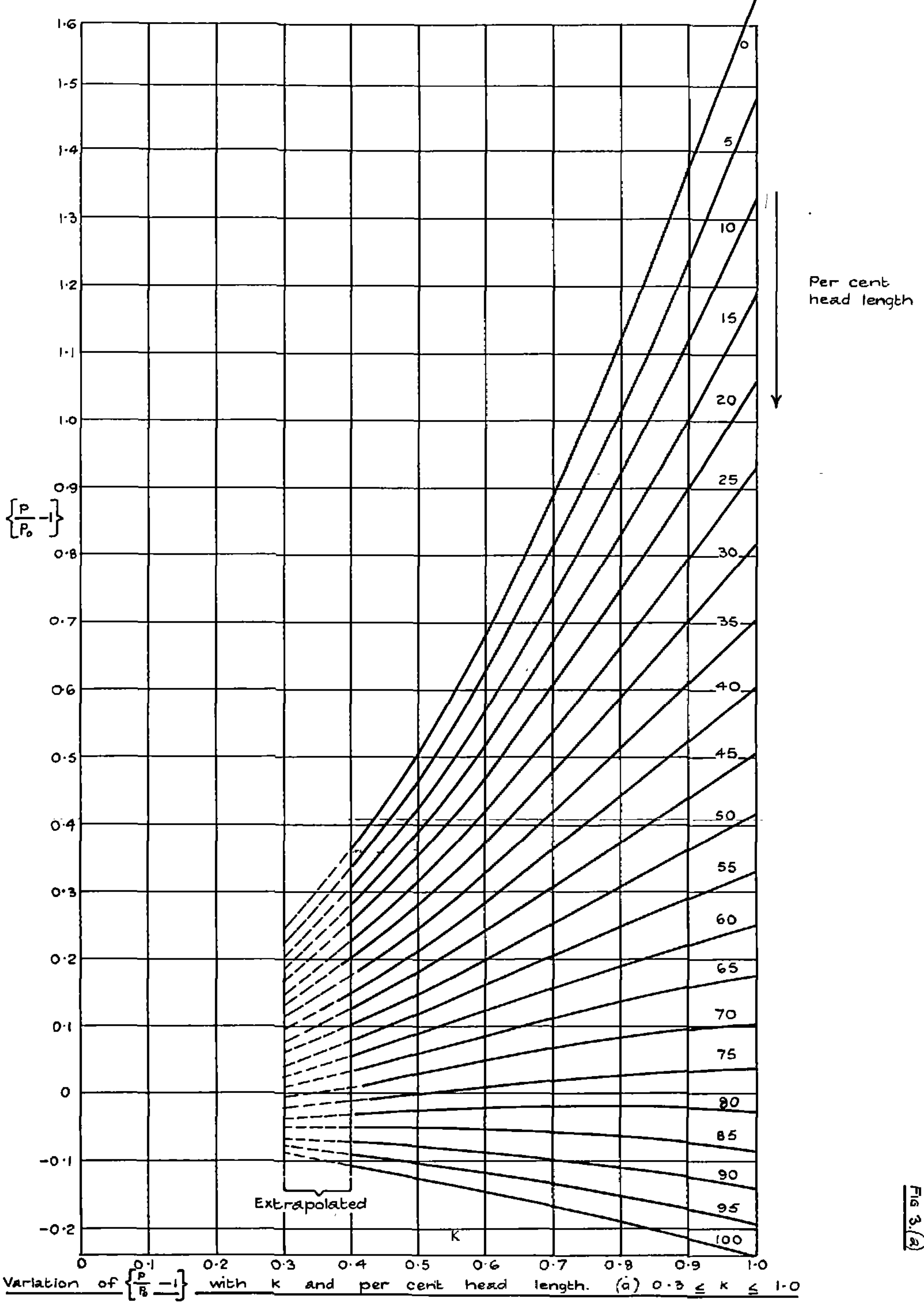
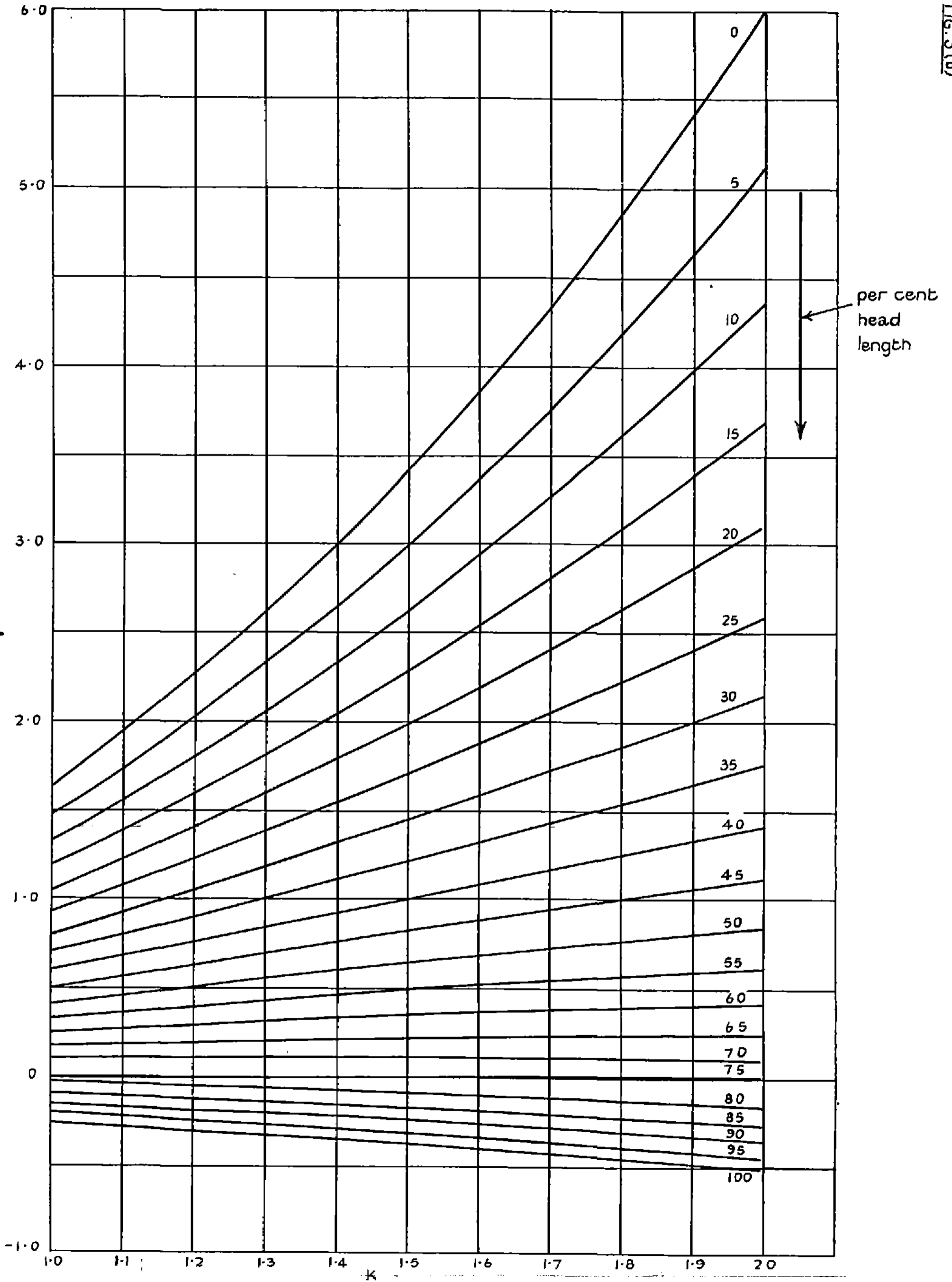
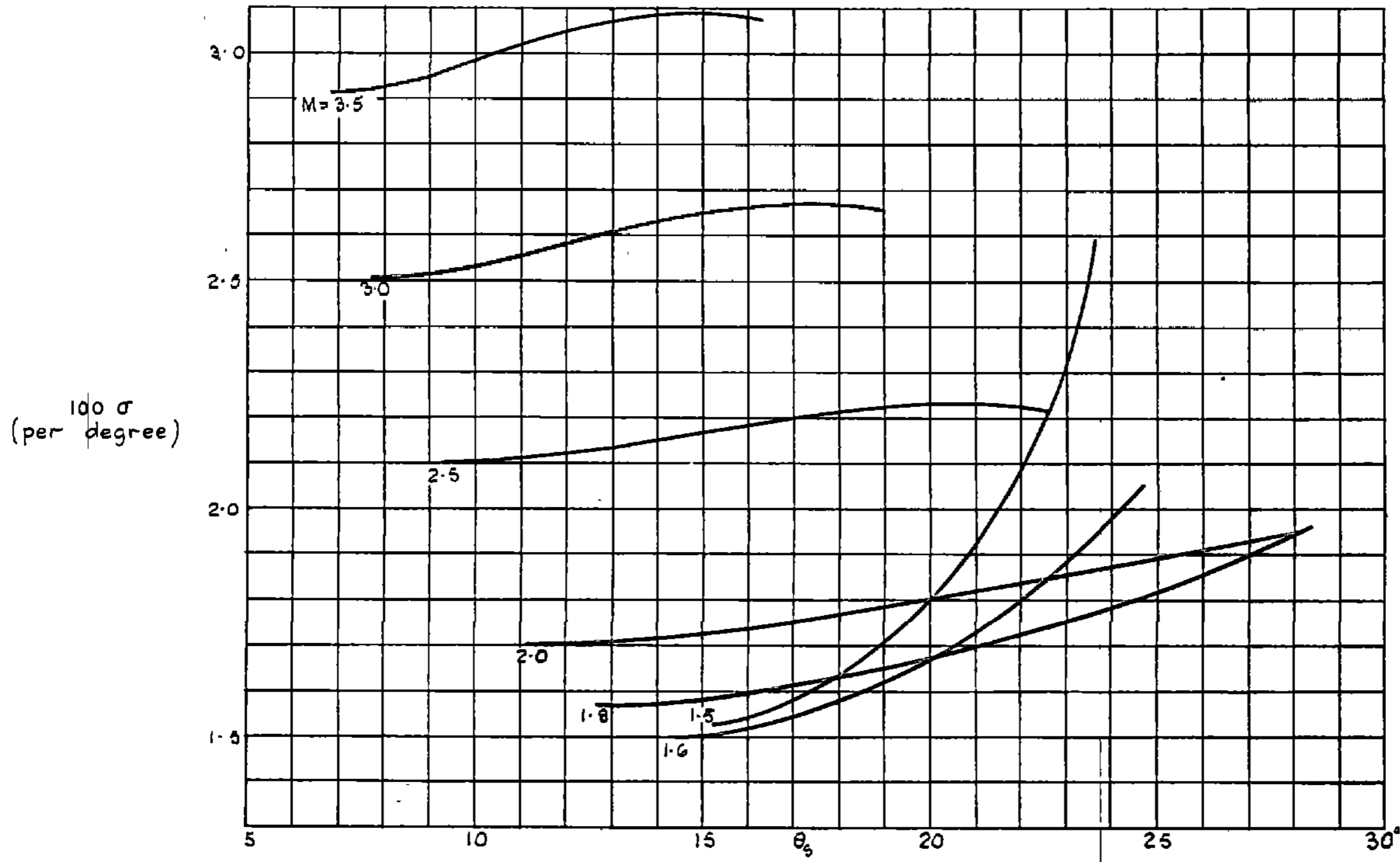


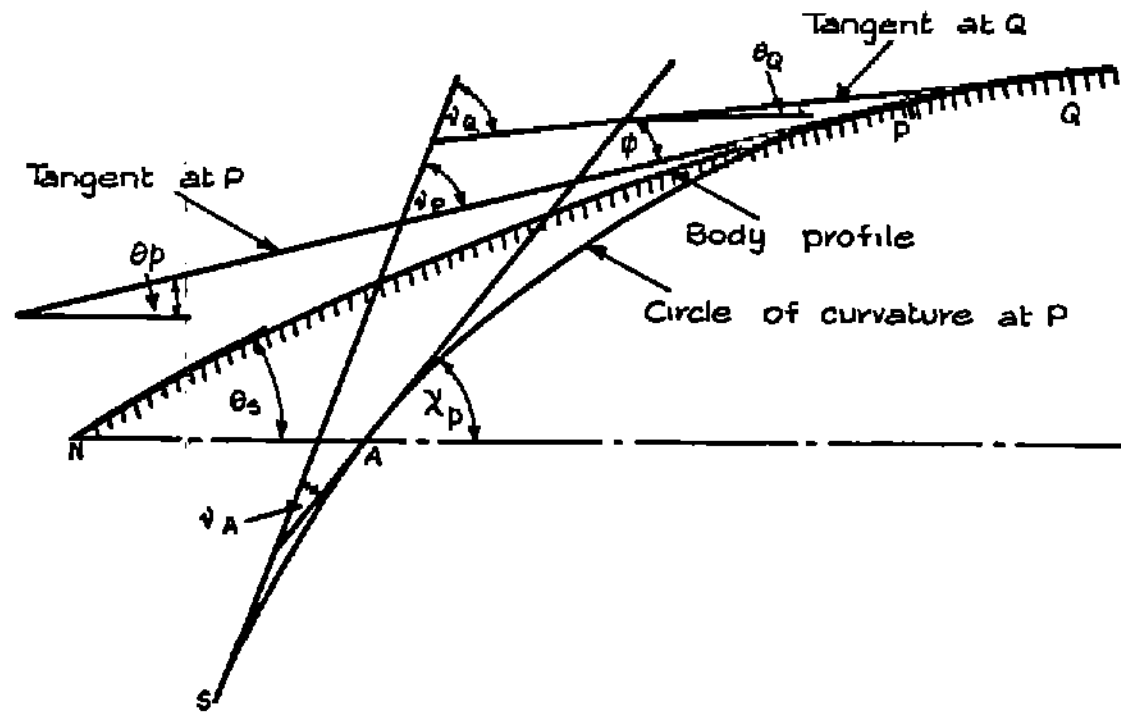
Fig 3(a)



(b) $1.0 \leq K \leq 2.0$
 $\left\{ \frac{p}{p_0} - 1 \right\}$

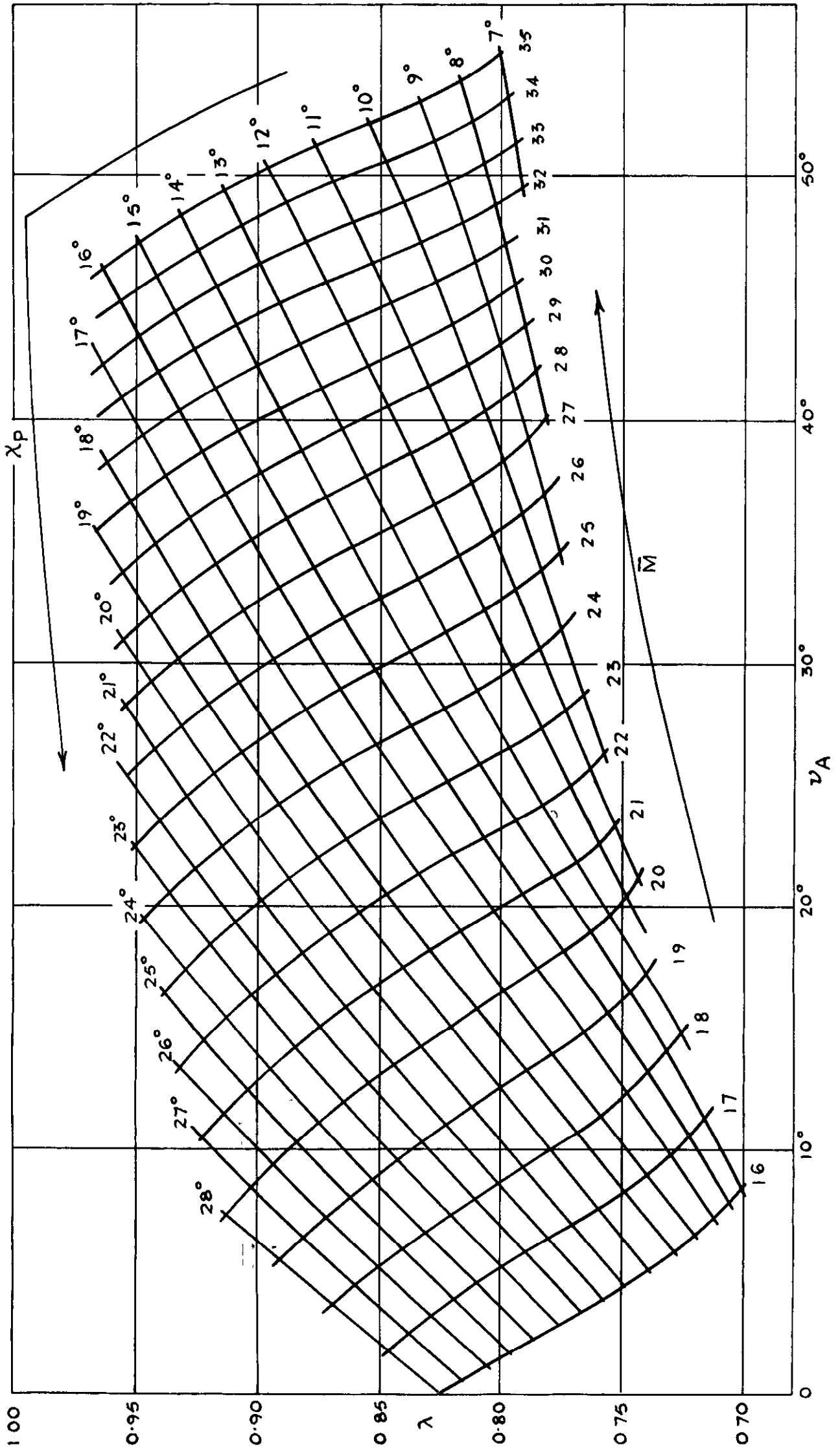


Variation of σ with θ_6 and M .



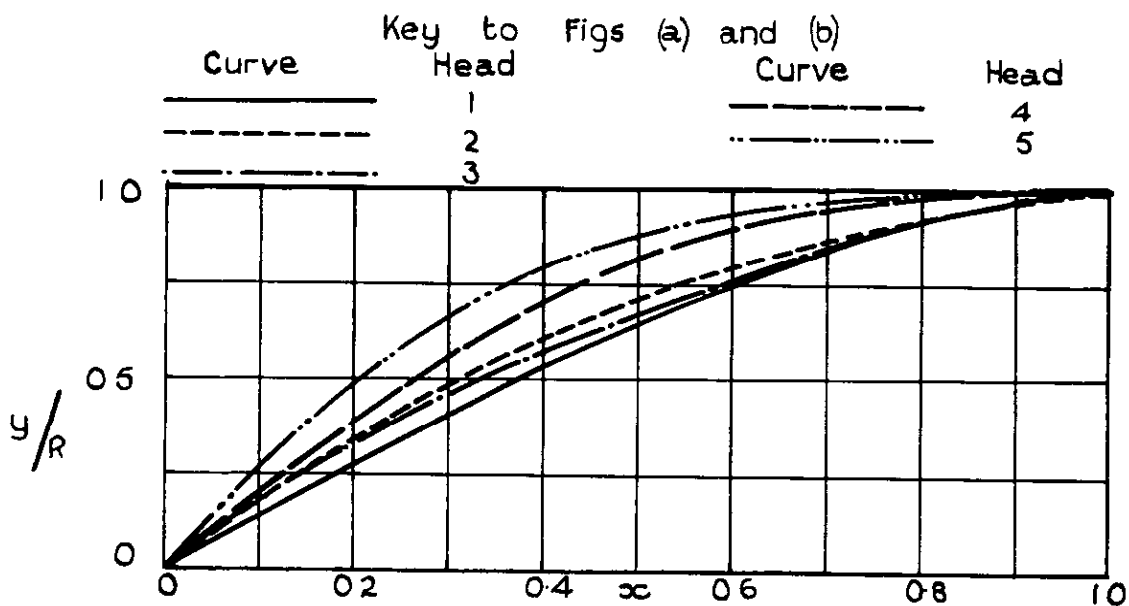
Geometry of supersonic flow past an arbitrary body

FIG. 6

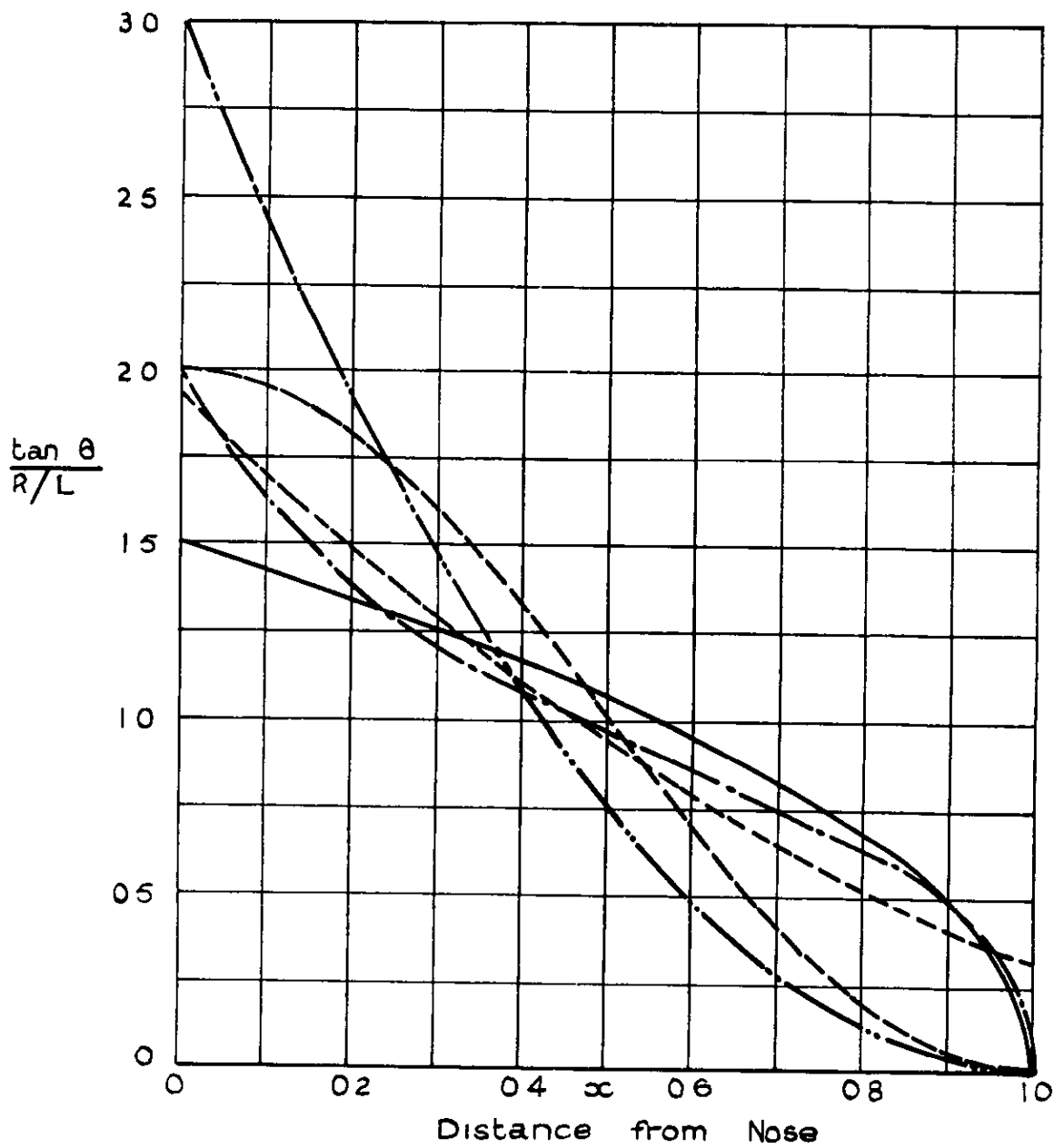


Variation of λ with ν_A and χ_p , with contours of constant \bar{M} shown

FIG 7 (a) (b)

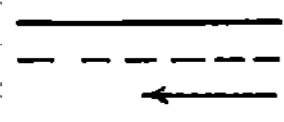


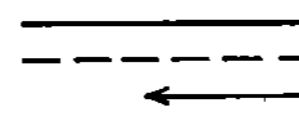
(a) Profiles

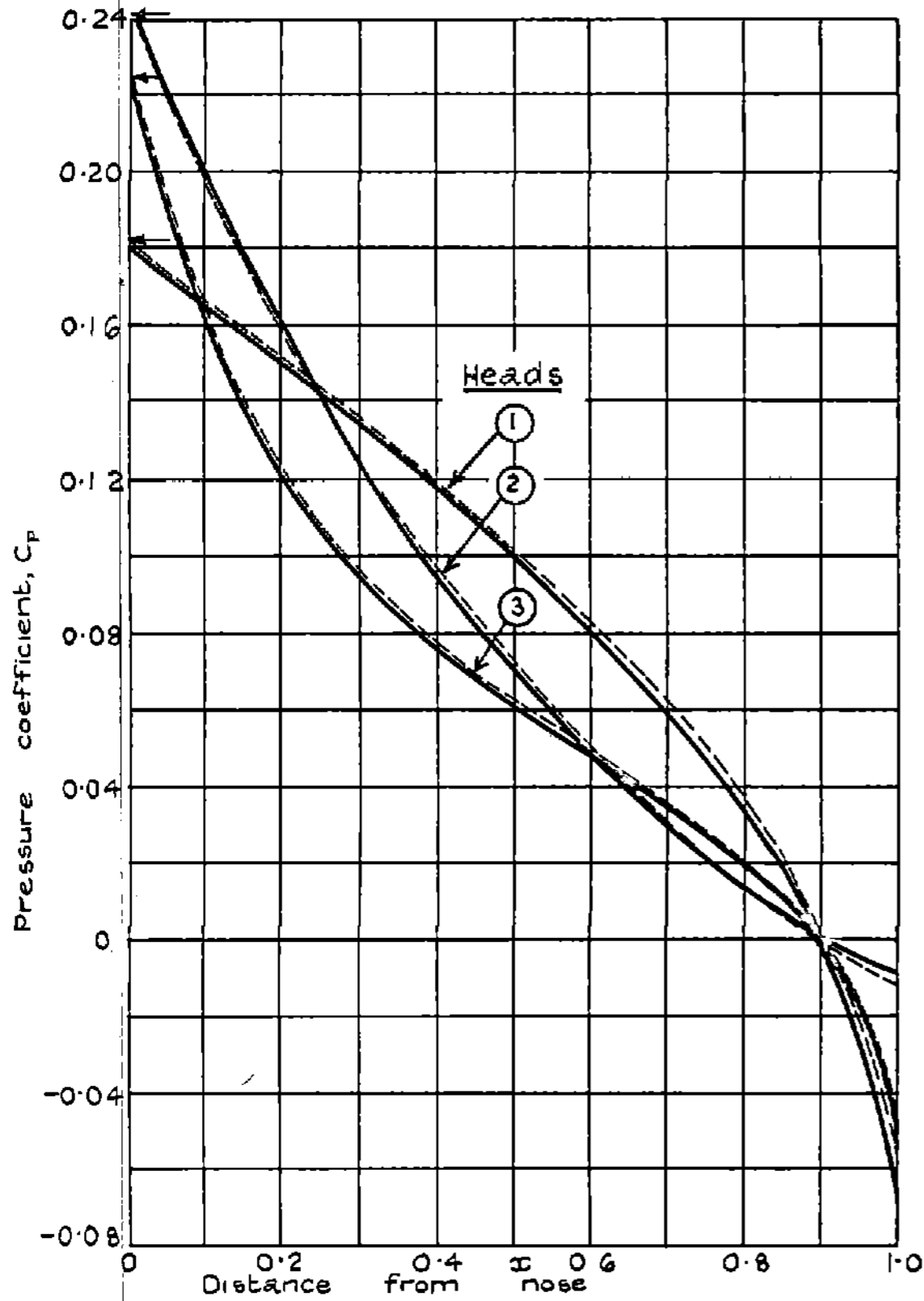


(b) Slope Distributions

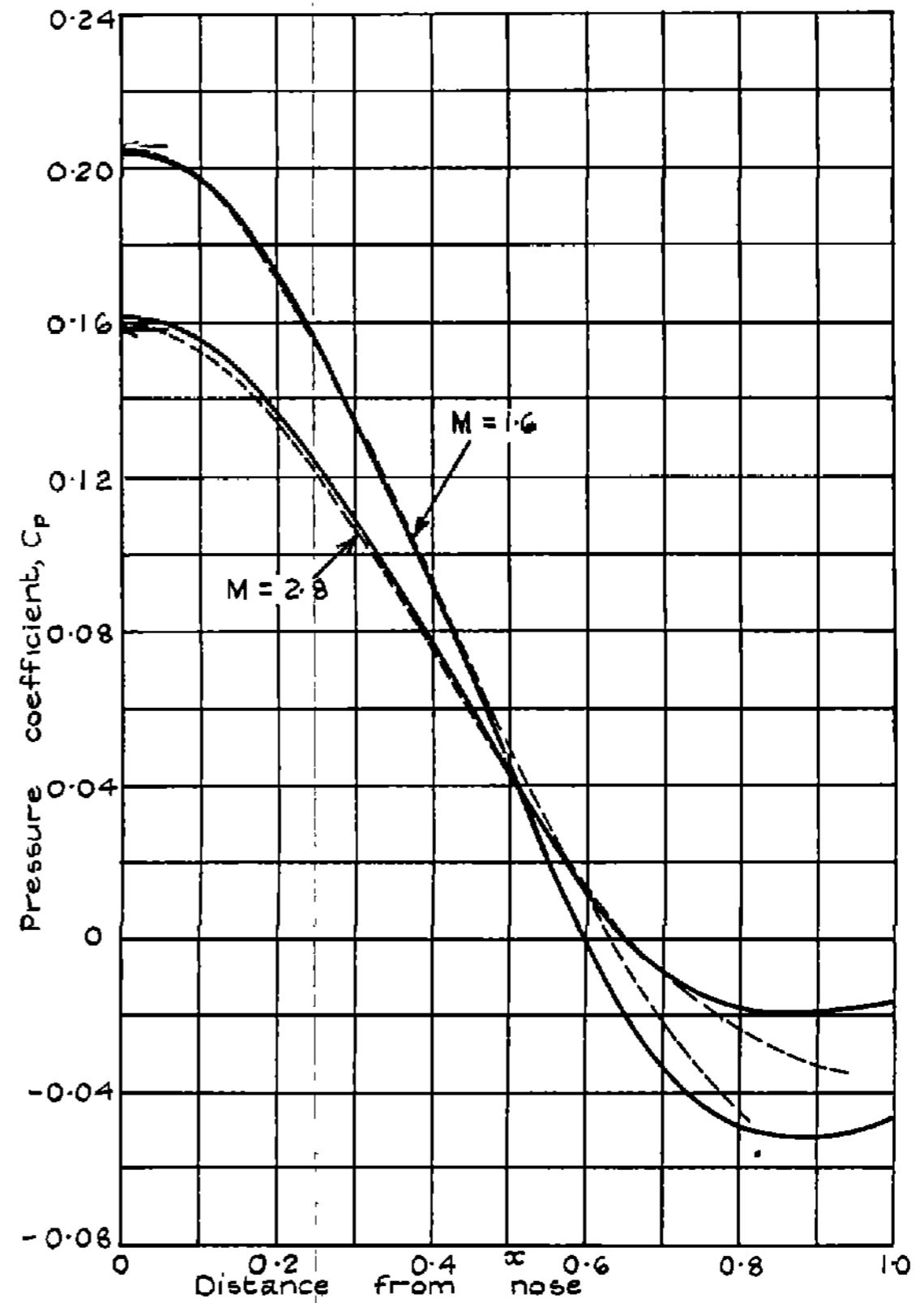
Geometric Characteristics of Heads 1 to 5.


 Van Dyke's method
 Step - by - step method
 Exact nose values (Taylor-Maccoll)


 Van Dyke's method
 Step - by - step method
 Exact nose values (Taylor-Maccoll)



(a) Heads 1, 2 and 3 at $M = 2.0$



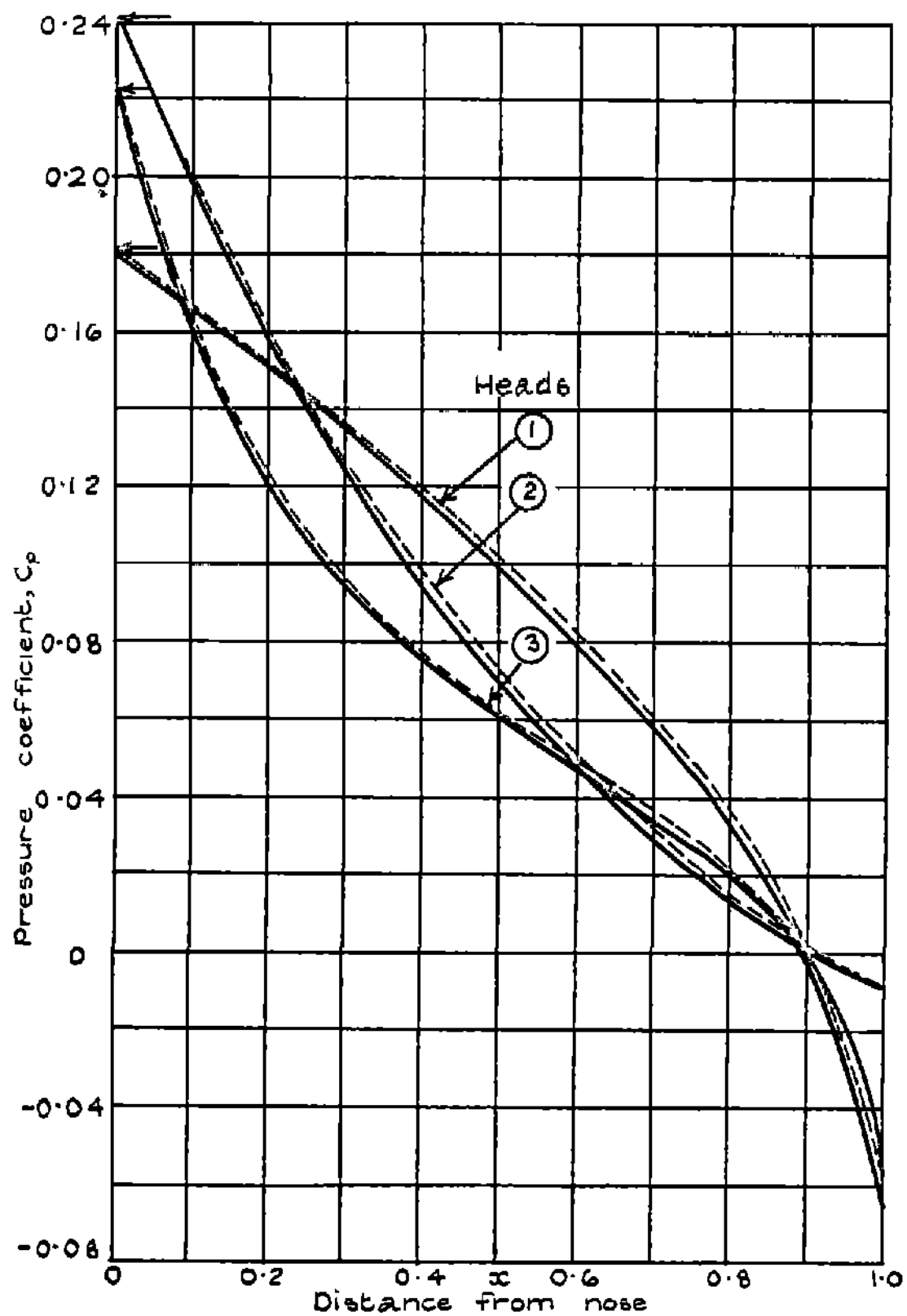
(b) Head 4 at $M = 1.6$ and $M = 2.8$

Pressure distributions by the step-by-step method.

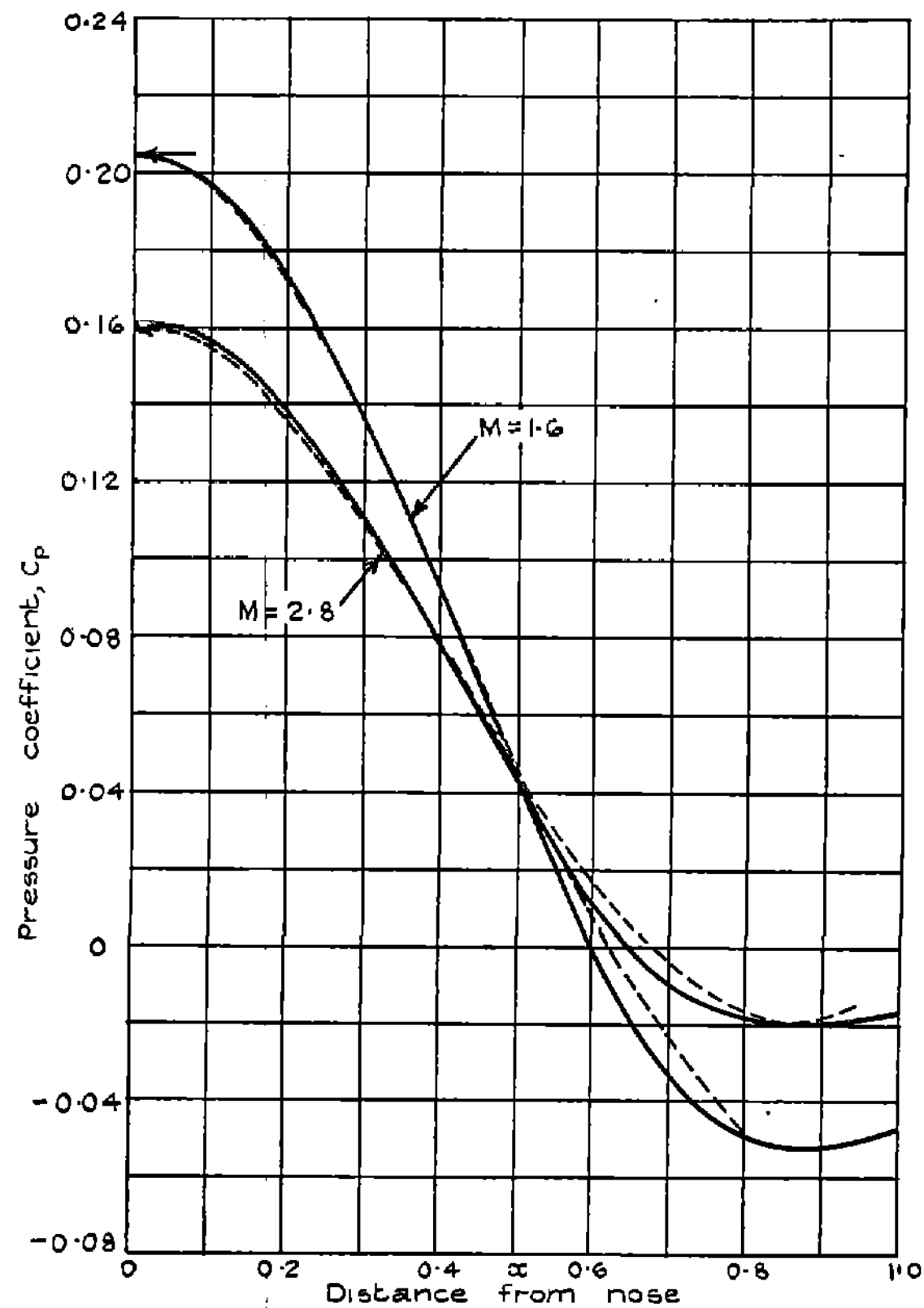
FIG 9.

_____ Van Dyke's method
 - - - - - Ogive of curvature method
 ← Exact nose values (Taylor-Maccoll)

_____ Van Dyke's method
 - - - - - Ogive of curvature method
 ← Exact nose values (Taylor-Maccoll)



(a) Heads 1, 2 and 3 at $M=2.0$

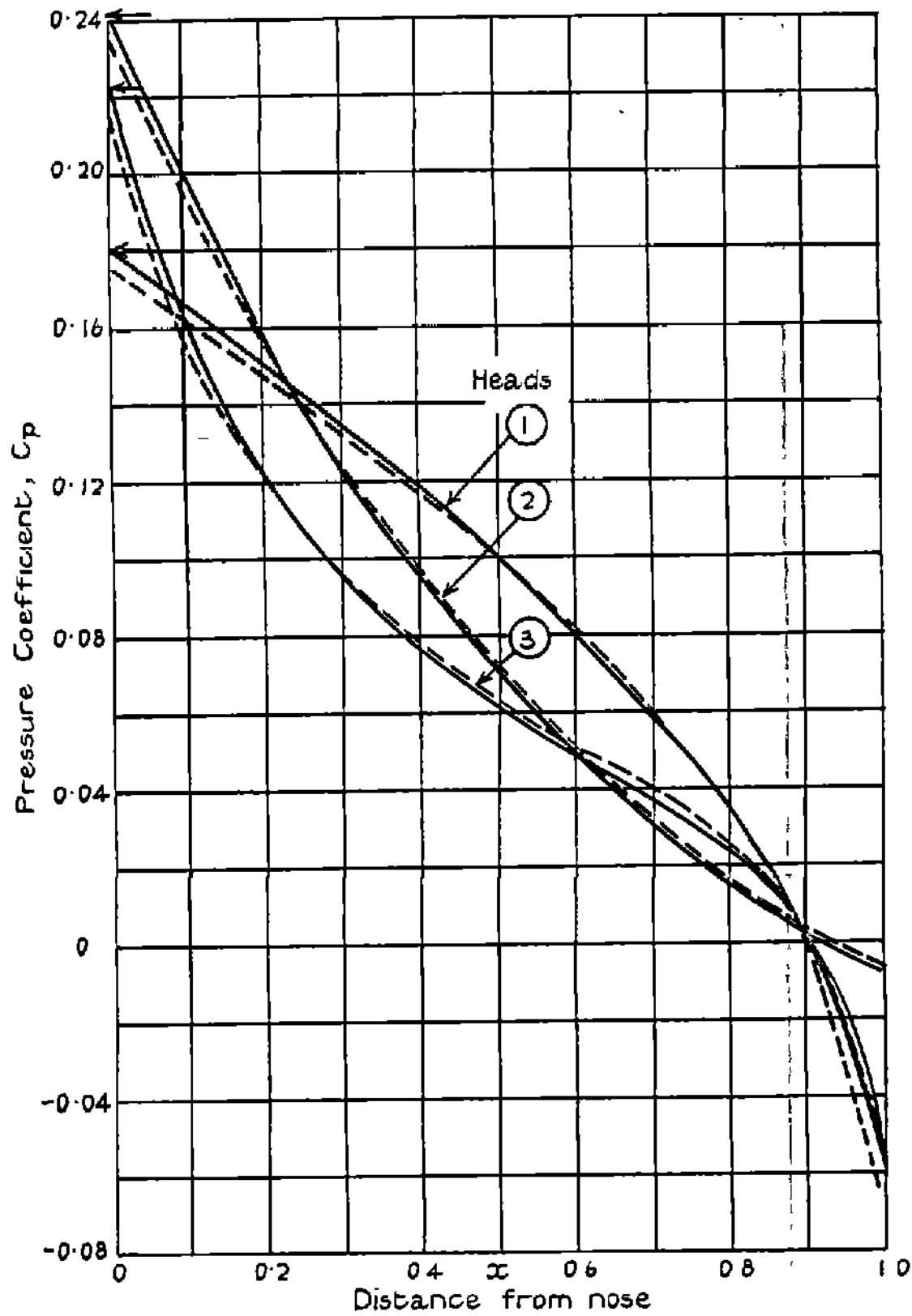


(b) Head 4 at $M=1.6$ and $M=2.8$

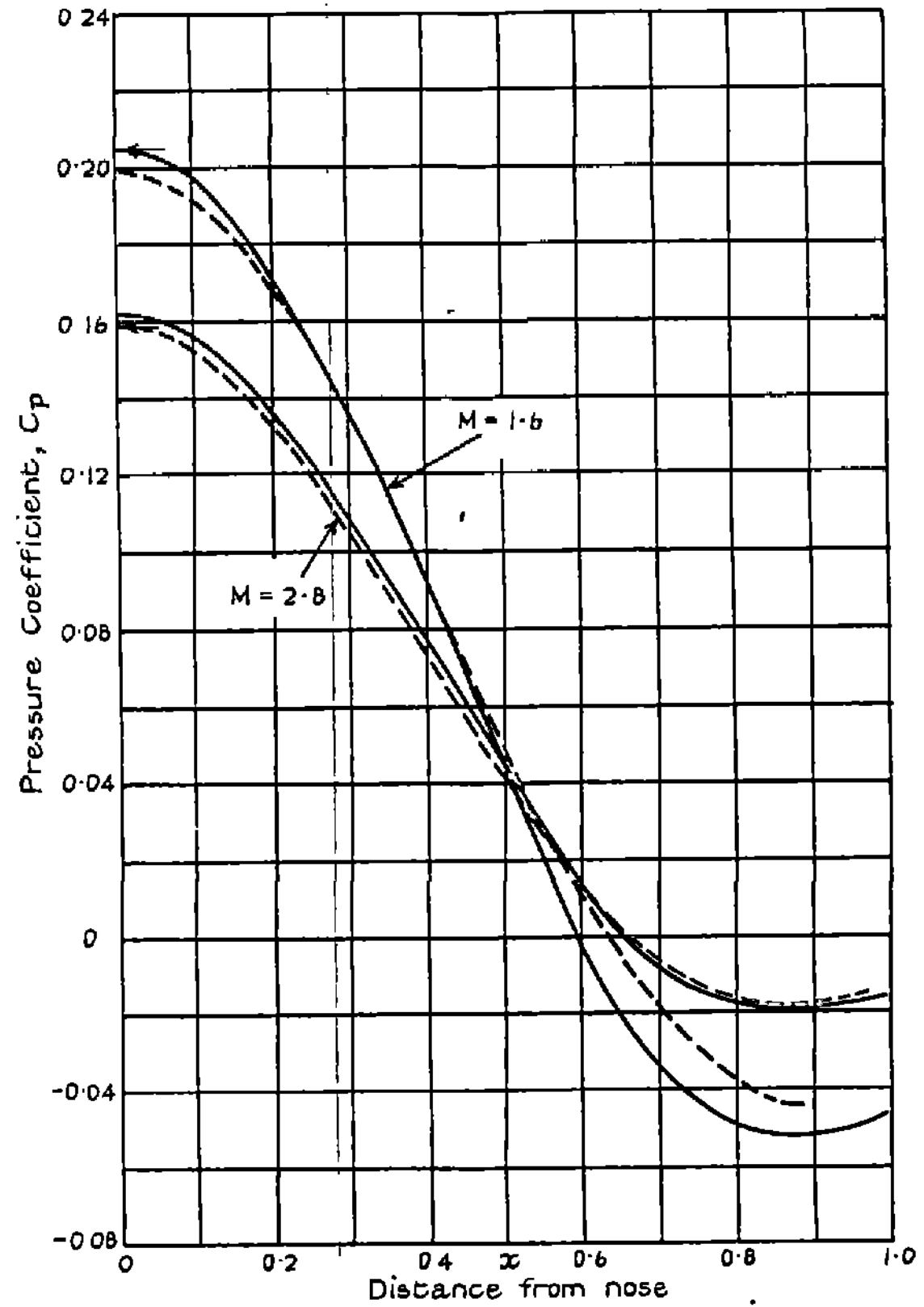
Pressure distributions by the ogive of curvature method using L.A.E 024 (Ref. 4).

————— Van Dyke's method
 - - - - - Ogive of curvature method using NACA TN 2250 (Ref 6).
 ← Exact nose values (Taylor - Maccoll)

————— Van Dyke's method
 - - - - - Ogive of curvature method using NACA TN 2250 (Ref. 6).
 ← Exact nose values (Taylor - Maccoll)



(a) Heads 1, 2 and 3 at $M=20$



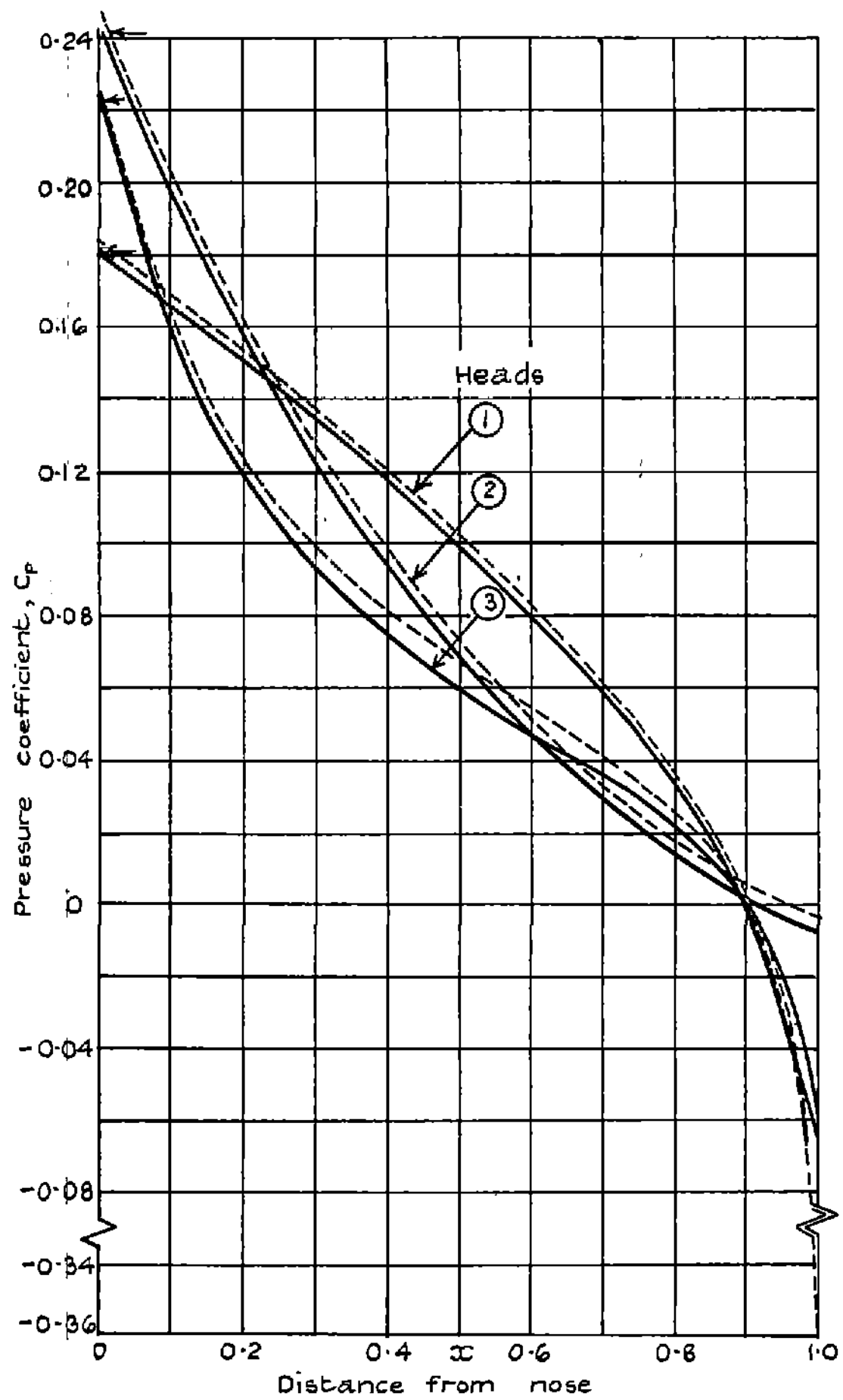
(b) Head 4 at $M=1.6$ and $M=2.8$

Pressure Distributions by the ogive of curvature method using NACA TN 2250 (Ref 6)

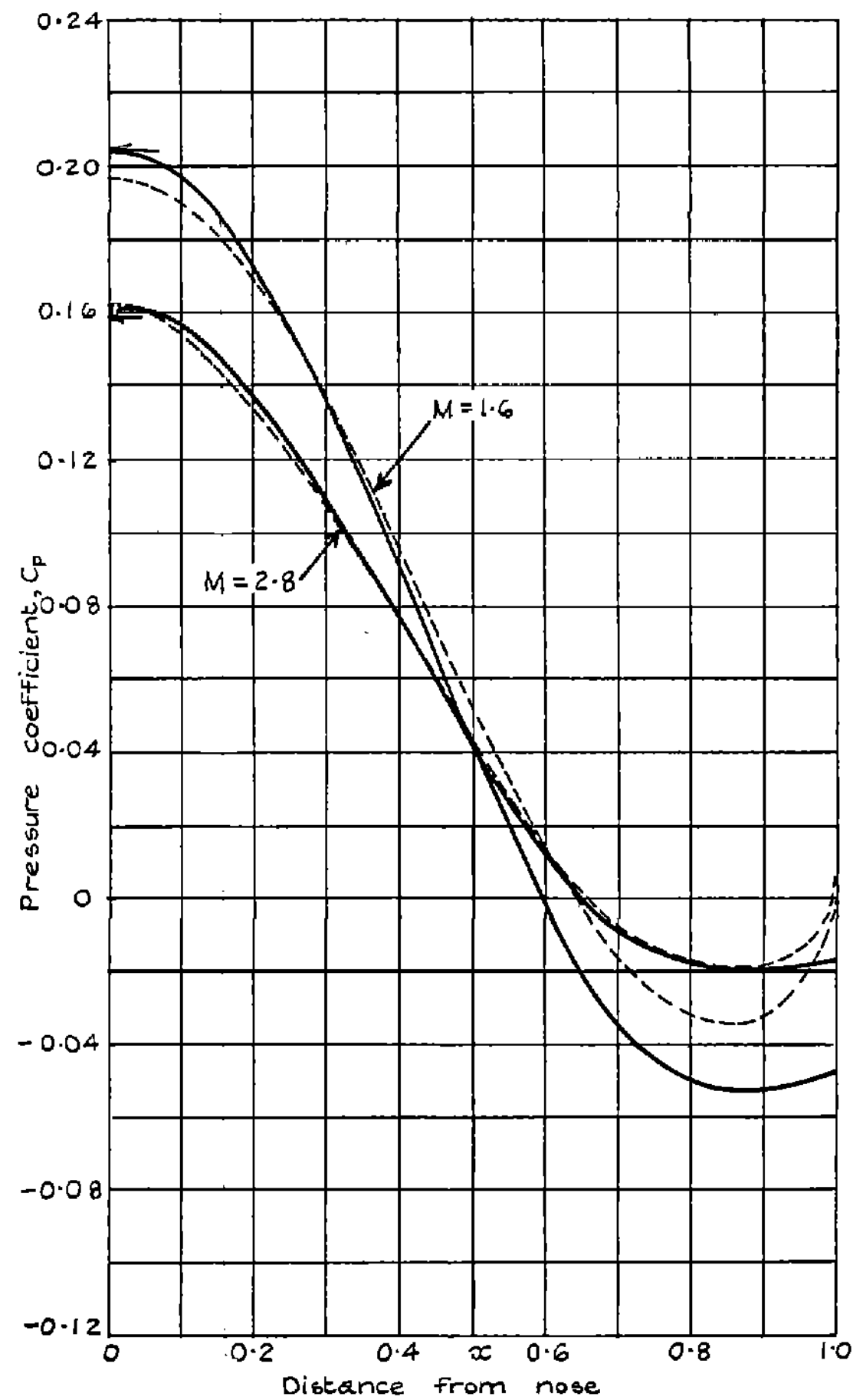
FIG II.

————— Van Dyke's method
 - - - - - Derivative formula
 ← ← ← Exact nose values (Taylor-Maccoll)

————— Van Dyke's method
 - - - - - Derivative formula
 ← ← ← Exact nose values (Taylor - Maccoll)

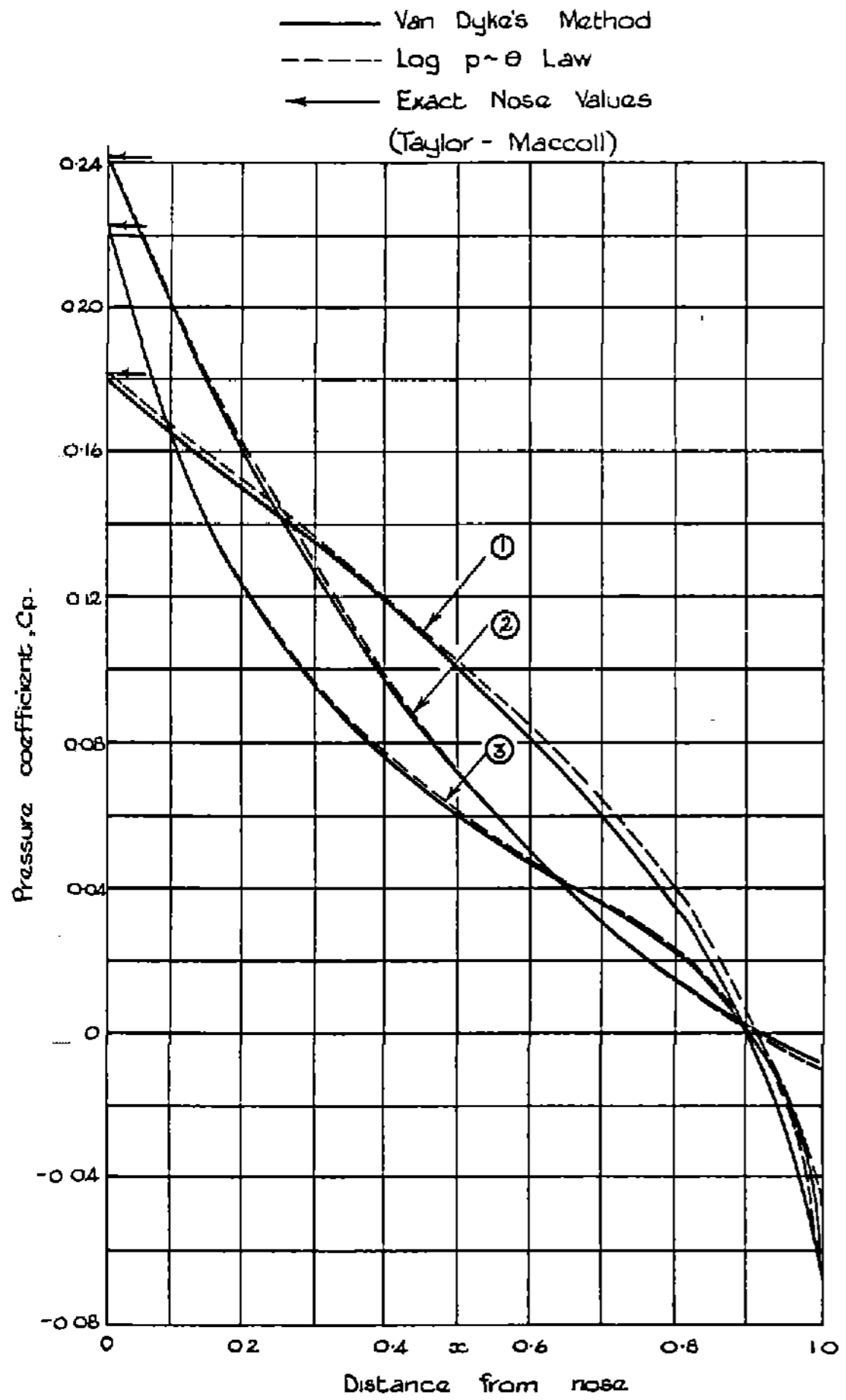


(a) Heads 1, 2 and 3 at $M=2.0$

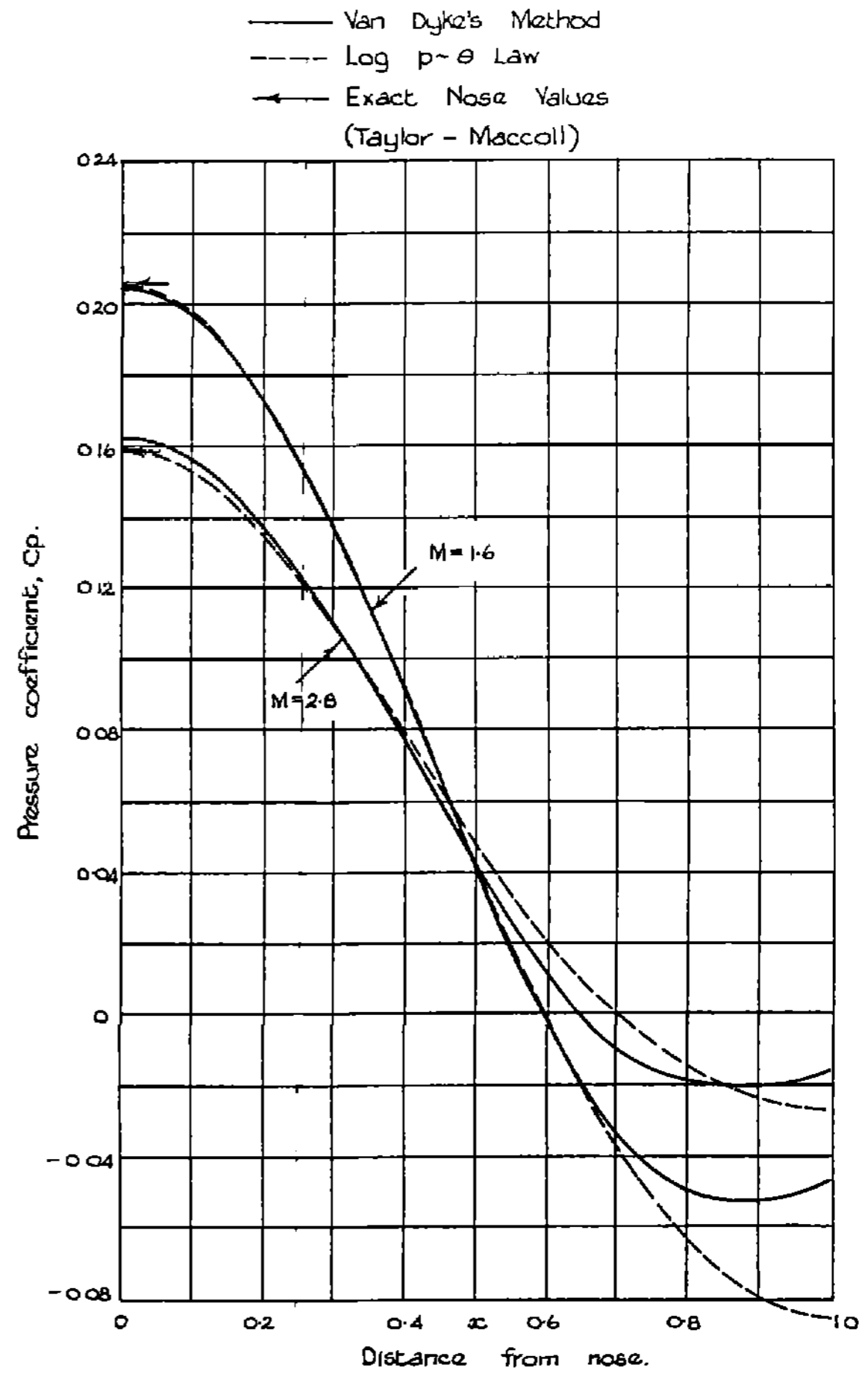


(b) Head 4 at $M=1.6$ and 2.8

Pressure distributions by the derivative formula.



(a) Heads 1, 2 and 3 at $M=2.0$.

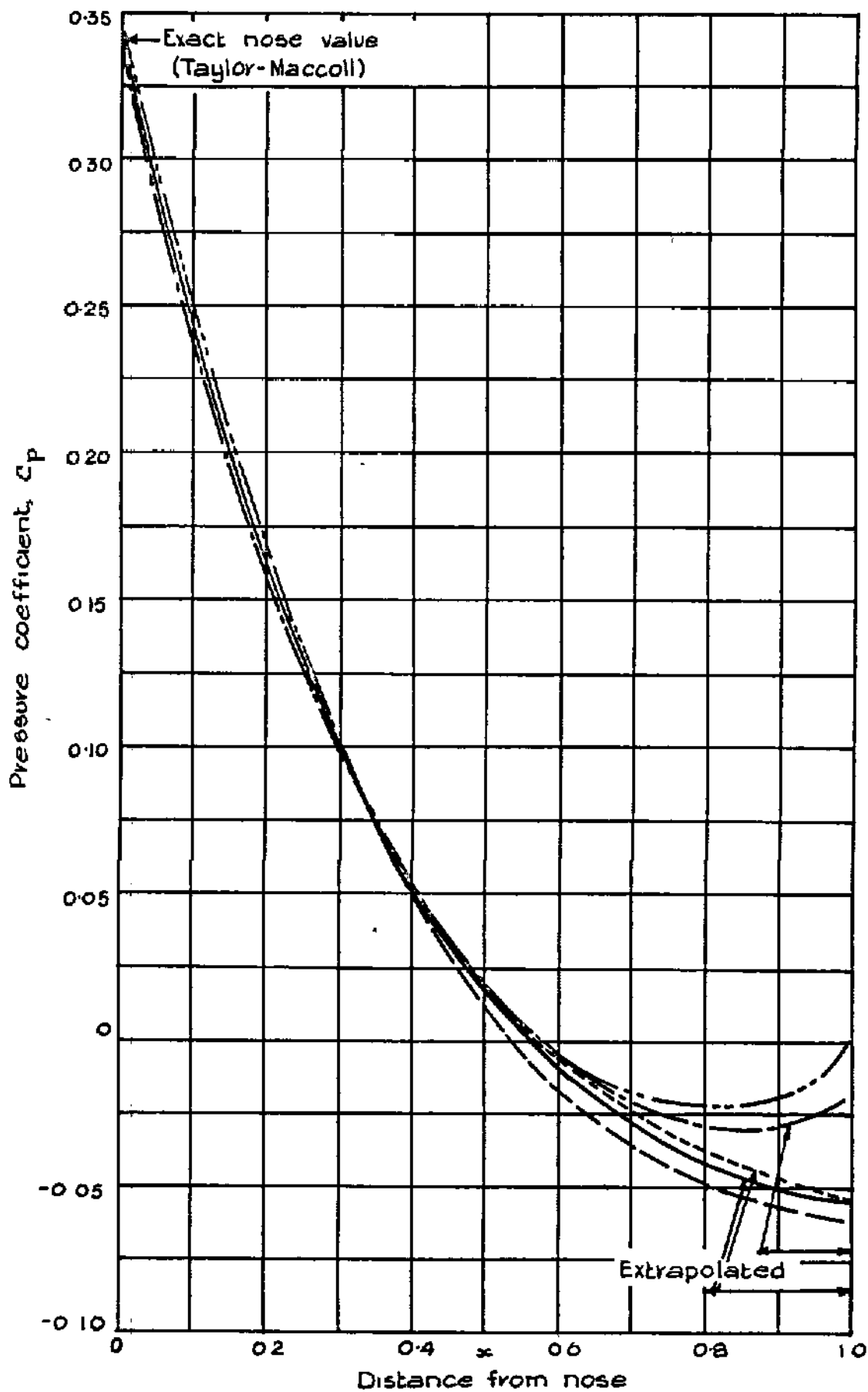


(b) Head 4 at $M=1.6$ and 2.8

Pressure Distributions by the Log $p \sim \theta$ Law

FIG. 13

Curve	Method
————	Step-by-step
-----	Ogive of curvature using LA 024
- - - - -	-Do- using NACA TN 2250
.....	Derivative formula
— · — · —	Log $p \sim \theta$ law.



Pressure distributions on head 5 at $M=2.0$ by the five methods.

CROWN COPYRIGHT RESERVED

PRINTED AND PUBLISHED BY HER MAJESTY'S STATIONERY OFFICE

To be purchased from

York House, Kingsway, LONDON, W C 2 423 Oxford Street, LONDON, W 1

P O Box 569, LONDON, S E 1

13a Castle Street, EDINBURGH, 2 1 St Andrew's Crescent, CARDIFF

39 King Street, MANCHESTER, 2 Tower Lane, BRISTOL, 1

2 Edmund Street, BIRMINGHAM, 3 80 Chichester Street, BELFAST

or from any Bookseller

1954

Price 5s 0d net

PRINTED IN GREAT BRITAIN